



HAL
open science

Control of *Clostridium difficile* Physiopathology in Response to Cysteine Availability.

Thomas Dubois, Marie Dancer-Thibonnier, Marc Monot, Audrey Hamiot, Laurent Bouillaut, Olga Soutourina, Isabelle Martin-Verstraete, Bruno Dupuy

► **To cite this version:**

Thomas Dubois, Marie Dancer-Thibonnier, Marc Monot, Audrey Hamiot, Laurent Bouillaut, et al.. Control of *Clostridium difficile* Physiopathology in Response to Cysteine Availability.. *Infection and Immunity*, 2016, 84 (8), pp.2389-405. 10.1128/IAI.00121-16 . pasteur-01370880

HAL Id: pasteur-01370880

<https://pasteur.hal.science/pasteur-01370880v1>

Submitted on 23 Sep 2016

HAL is a multi-disciplinary open access archive for the deposit and dissemination of scientific research documents, whether they are published or not. The documents may come from teaching and research institutions in France or abroad, or from public or private research centers.

L'archive ouverte pluridisciplinaire **HAL**, est destinée au dépôt et à la diffusion de documents scientifiques de niveau recherche, publiés ou non, émanant des établissements d'enseignement et de recherche français ou étrangers, des laboratoires publics ou privés.

Copyright

1 **Control of *Clostridium difficile* physiopathology in response to cysteine availability**

2

3 **Thomas Dubois^{1#}, Marie Dancer-Thibonnier^{1#}, Marc Monot¹, Audrey Hamiot¹,**
4 **Laurent Bouillaut³, Olga Soutourina^{1,2}, Isabelle Martin-Verstraete^{1,2,#} and Bruno**
5 **Dupuy^{1, #,*}**

6

7 1. Laboratoire Pathogénèse des Bactéries Anaérobies, Institut Pasteur, 25-28, rue du
8 Docteur Roux, 75724 Paris Cedex 15, France.

9 2. Université Paris 7-Denis Diderot, 75205 Paris, France

10 3. Department of Molecular Biology and Microbiology, Tufts University School of
11 Medicine, Boston, MA, USA

12

13 # These authors contributed equally to this work

14

15

16 Corresponding author: Bruno Dupuy *

17 E-mail: bdupuy@pasteur

18

19 **Key words:** cysteine metabolism, iron sulfur cluster, oxidative stress, fermentation

20

21 **Running title:** *C. difficile* toxin regulation by cysteine

22

23

24 **Abstract**

25 The pathogenicity of *Clostridium difficile* is linked to its ability to produce two toxins:
26 TcdA and TcdB. The level of toxin synthesis is influenced by environmental signals, such
27 as PTS sugars, biotin and amino acids, especially cysteine. To understand the molecular
28 mechanisms of cysteine-dependent repression of toxin production, we reconstructed the
29 sulfur metabolism pathways of *C. difficile* strain 630 *in silico* and validated some of them
30 by testing *C. difficile* growth in the presence of various sulfur sources. High levels of
31 sulfide and pyruvate were produced in the presence of 10 mM cysteine, indicating that
32 cysteine is actively catabolized by cysteine desulfhydrases. Using a transcriptomic
33 approach, we analyzed cysteine-dependent control of gene expression and showed that
34 cysteine modulates the expression of genes involved in cysteine metabolism, amino-acid
35 biosynthesis, fermentation, energy metabolism, iron acquisition and the stress response.
36 Additionally, sigma factor (SigL) and global regulators (CcpA, CodY, Fur) were tested to
37 elucidate their roles in the cysteine-dependent regulation of toxin production. Among
38 these regulators, only *sigL* inactivation resulted in the de-repression of toxin-gene
39 expression in the presence of cysteine. Interestingly, the *sigL* mutant produced less
40 pyruvate and H₂S than the wild-type strain. Unlike cysteine, the addition of 10 mM
41 pyruvate to the medium for a short time during the growth of the wild-type and *sigL*
42 mutant strains reduced expression of the toxin gene, indicating that cysteine-dependent
43 repression of toxin production is mainly due to the accumulation of cysteine by-products
44 during growth. Finally, we showed that the effect of pyruvate on toxin-gene expression is
45 mediated at least in part by the two-component system CD2602-CD2601.

46

47 **Introduction**

48

49 *Clostridium difficile* is a Gram-positive spore-forming obligate anaerobe and the major
50 cause of nosocomial diarrhea associated with antibiotic therapy. The symptoms of *C.*
51 *difficile* infection (CDI) vary from mild diarrhea to life-threatening pseudomembranous
52 colitis, a severe form of CDI (1). Virulent *C. difficile* strains produce two large toxins, an
53 enterotoxin (TcdA) and a cytotoxin (TcdB). The *tcdA* and *tcdB* genes are clustered within
54 a single chromosomal region called the pathogenicity locus (PaLoc) with three accessory
55 genes, *tcdR*, *tcdE* and *tcdC*. The expression of the toxin genes is controlled through the
56 coordinated action of the alternative sigma factor TcdR and its antagonist factor TcdC (2-
57 4). The *tcdE* gene encodes a holin-like protein that is required for toxin release (5).

58

59 The spectrum of diseases caused by *C. difficile* depends on host factors and, for the severe
60 forms, on the level of toxins produced, suggesting that the regulation of toxin synthesis is
61 a critical determinant of *C. difficile* pathogenicity (6). Toxin production starts when *C.*
62 *difficile* cultures enter the stationary growth phase (7) and is modulated in response to
63 various environmental signals. Exposure to subinhibitory concentrations of antibiotics, a
64 temperature of 37°C, biotin limitation or the presence of butyric acid stimulates toxin
65 production (8, 9). By contrast, the presence of rapidly metabolized carbon sources, such
66 as glucose and butanol, or amino acids, such as cysteine and proline, inhibit toxin
67 synthesis (7, 10-12). Some of the molecular mechanisms regulating *C. difficile* toxin
68 synthesis in response to environmental signals have been elucidated (13-16). It has been
69 shown that CodY, the global regulator involved in the adaptive response to nutrient
70 limitation, represses toxin-gene expression by binding to the *tcdR* promoter region (14,
71 17) and that glucose-dependent repression of toxin production is mediated by CcpA, the
72 global regulator of carbon catabolite repression (CCR) (13). This repression is the result
73 of the direct binding of CcpA to a *cis*-acting catabolite response element (*cre* site) that is
74 present in the regulatory regions of the *tcdA*, *tcdB*, *tcdR* and *tcdC* genes, with the strongest
75 affinity observed for the *tcdR* promoter (18). Toxin-gene expression also depends on
76 transcriptional factors, such as SigH and Spo0A, which control the transition to the post-
77 exponential growth phase and the initiation of sporulation (15, 16).

78 Changes in colonic flora after antibiotic treatment lead to the modification of
79 metabolic pools, which affects the spore germination and cell growth of *C. difficile* (19).

80 Specifically, the levels of several PTS sugars, such as mannitol and sorbitol, and amino
81 acids, such as proline, cysteine and cystine, the cysteine dimer, increase during gut
82 dysbiosis. These compounds are metabolized by *C. difficile* and may serve as metabolic
83 signals that are detected by regulators to coordinate adaptation, growth and virulence-
84 factor production during gut colonization.

85 Among the amino acids that down-regulate toxin production in *C. difficile* strains, cysteine
86 is the most potent (11, 12). Links between bacterial virulence and cysteine metabolism
87 have been described in several pathogenic bacteria. In *Clostridium perfringens* and
88 *Bordetella pertussis*, toxin synthesis is regulated in response to cysteine availability (20,
89 21). Additionally, genes involved in sulfur metabolism are induced when *Mycobacterium*
90 *tuberculosis*, *Yersinia ruckeri*, *Staphylococcus aureus* and *Nesseiria meningitidis* interact
91 with human cells (22-24). In addition, loss-of-function mutations in genes involved in
92 cysteine biosynthesis or degradation affect the virulence for some of these pathogens (23-
93 26). Finally, the master regulator of cysteine metabolism in *S. aureus*, CymR, plays an
94 important role in both the stress response and the control of bacterial virulence (27).

95 The sulfur-containing amino acid cysteine is central to bacterial physiology. This
96 amino acid is a precursor of methionine and of several co-enzymes (biotin, thiamine,
97 coenzyme A and coenzyme M). Cysteine is also the sulfur donor for the biogenesis of the
98 iron-sulfur (Fe-S) clusters that are found in the catalytic site of several enzymes and
99 assists in protein folding and assembly by forming disulfide bonds. Moreover, cysteine-
100 containing proteins (thioredoxin, glutaredoxin) and molecules (glutathione, bacillithiol,
101 mycothiol) are important in protecting cells against oxidative stress (28, 29). Two major
102 cysteine biosynthetic pathways are present in microorganisms: i) the thiolation pathway,
103 which directly incorporates sulfide or thiosulfate into *O*-acetyl-L-serine (OAS), and ii) the
104 reverse transsulfuration pathway, which converts homocysteine into cysteine via a
105 cystathionine intermediate (Fig. 1) (30, 31). Homocysteine is synthesized from
106 methionine using the S-adenosyl-methionine (SAM) recycling pathway, while sulfide
107 arises mostly from the reduction of sulfate.

108 Due to the reactivity of its thiol group, the intracellular concentration of cysteine
109 must be tightly controlled. The pathways responsible for depleting free cysteine include
110 those that incorporate cysteine into molecules (proteins, methionine, Fe-S clusters,
111 vitamins) and those that degrade or export it (30). Cysteine can also be catabolized by
112 cysteine desulfhydrases or cysteine desulfidase, producing pyruvate and hydrogen sulfide

113 (H₂S) (Fig. 1) (24, 32). Finally, a large variety of molecular mechanisms participate in fine-
114 tuning cysteine metabolism in response to environmental changes. These systems include
115 regulation by the premature termination of transcription at T-box systems in response to
116 the level of charge of tRNA_{Cys} (33) or by several transcriptional regulators, including
117 activators of the LysR family (30) and CymR, a repressor of the Rrf2-family (34, 35).

118

119 To understand the molecular mechanisms involved in the cysteine response, we
120 performed a reconstruction of *C. difficile* sulfur metabolism and analyzed the global effect
121 of cysteine on gene expression. Then, we showed that cysteine-dependent repression of
122 toxin production requires SigL. Moreover, we observed that the production of pyruvate
123 and H₂S decreased in the *sigL* mutant compared to the wild-type strain. Interestingly,
124 addition of pyruvate to the growth medium of the wild-type and the *sigL* mutant strains
125 repressed toxin-gene transcription, suggesting that the effect of cysteine on toxin
126 production is due, at least in part, to the accumulation of cysteine by-products resulting
127 from cysteine degradation. Finally, we showed that the regulation of toxins by exogenous
128 pyruvate is mediated by a two-component system (TCS) through a still uncharacterized
129 mechanism.

130

131 **Materials and Methods**

132

133 **Bacterial strains and culture conditions**

134 The *C. difficile* strains used in this study are described in Table 1. *Escherichia coli* strain
135 NEB-10 beta (BioLabs) and *E. coli* strain HB101 (RP4) were used, respectively, for cloning
136 and as a donor strain for *C. difficile* conjugation experiments. *C. difficile* strains were
137 grown anaerobically (5% H₂, 5% CO₂, 90% N₂) in PY (Bacto peptone (20g/l); Yeast extract
138 (10g/l); CaCl₂ 0.4% (2ml/l); Resazurine 0.025% (4m/l); Hemin 0.05% (10ml/l); Vitamin
139 K 0.05% (1m/l) and 40ml/l of salts solution (K₂HPO₄ (1g/l), KH₂PO₄ (1g/l), NaHCO₂
140 (10g/l), NaCl (2g/l), MgSO₄·7H₂O (0.2g/l)), PYC (PY with 10 mM cysteine) or PYHC (PY
141 with 10 mM homocysteine) media (12). After 9 h of cell growth, 15 mM of acetate or 10
142 mM of pyruvate, Na₂S or formate were added to the PY medium. When necessary,
143 cefoxitin (25 µg/ml), thiamphenicol (15 µg/ml) or erythromycin (2.5 µg/ml) were added
144 to *C. difficile* cultures. *E. coli* strains were grown in Luria-Bertani (LB) broth. When
145 indicated, ampicillin (100 µg/ml) or chloramphenicol (15 µg/ml) was added to the

146 culture medium. Additionally, 200 ng/ml of anhydrotetracycline (Atc) was used to induce
147 the *P_{tet}* promoter of the pRPF185 vector derivatives in *C. difficile* (36). The sulfur-free
148 minimal medium was as previously described (20), with the addition of 0.3 g/L of proline.
149 The concentrations of the sulfur sources added are indicated in Table 2.

150 **Dot-blot analysis**

151 Crude extracts were obtained using the FastPrep® (MP Biomedicals) cell-lysis system
152 (speed 6, time 40, performed twice), followed by centrifugation (10 min at 4°C) to remove
153 cell debris. For dot-blot experiments, 20 ng (VPI10463) or 200 ng [630Δ*erm*, M7404 and
154 M7404 (*tcdC*⁺)] of proteins from the crude extracts were directly spotted onto a
155 nitrocellulose membrane (Hybond-C extra, Amersham Biosciences). The membranes
156 were blocked with 5% w/v non-fat dried milk in Tris-buffered saline (TBS) supplemented
157 with 0.2% (v/v) Tween-20 (TBST) for 1 h at room temperature (RT). The membranes
158 were then incubated for 90 min at 37°C with the TcdA antibody (PCG-4, Santa Cruz,
159 Biotechnology) and visualized as described by Antunes et al. (13).

160 **Cell cultures and cytotoxicity assays**

161 Vero cells were cultured in Dulbecco's modified Eagle's medium (DMEM; Gibco)
162 supplemented with 5% (v/v) fetal calf serum and a 1% ready-to-use solution (v/v) of
163 penicillin [10 000 U ml⁻¹] and streptomycin [10 mg ml⁻¹] (Sigma) at 37°C in 5% CO₂
164 atmosphere. For cytotoxicity assays, cells were grown until confluence in 96-well plates
165 and incubated with two-fold serially diluted *C. difficile* crude extracts in DMEM. After 24 h
166 at 37°C, the cytopathic effect was evaluated using an optical microscope. Positive toxin
167 reactions were indicated by the characteristic rounding of Vero cells. The titer of each
168 sample corresponds to the well containing 50 % round Vero cells.

169 **Detection and quantification of hydrogen-sulfide and pyruvate production**

170 H₂S production was detected using lead-acetate paper (Macherey-Nagel), which turns
171 black in the presence of this compound. Cells were grown in PY, PYC or PYHC to an
172 OD_{600nm} of 0.7. Then, the lead-acetate paper was placed at the bottom of the flask for 1
173 min to 1 h at 37°C, depending on the experiment. H₂S production was further quantified
174 as previously described (31, 37). Briefly, 5 ml of the 630Δ*erm* strain culture was
175 introduced into a flask with an alkaline agar layer enriched with zinc acetate and was
176 incubated for 1 h at 37°C. The OD_{670nm} was measured against an H₂O blank. The amount of

177 H₂S was calculated using a standard curve of Na₂S. For pyruvate quantification, cells were
178 grown in PY or PYC for 10 h at 37°C, and pyruvate was quantified in the supernatant using
179 a Pyruvate Assay Kit (Sigma). The final pyruvate concentration was standardized using
180 the OD_{600nm} of the bacterial cultures.

181 **Estimation of the intracellular amino-acid content**

182 The intracellular concentrations of amino acids were estimated using high-pressure liquid
183 chromatography (HPLC) (31, 38). Briefly, cells were suspended in a sulfosalicylic acid
184 buffer (3% final concentration) and disrupted using a Fastprep apparatus (MP
185 Biomedicals). After centrifugation, supernatant samples were analyzed by cation-
186 exchange chromatography, followed by ninhydrin postcolumn derivatization as
187 previously described (31).

188 **Zymogram**

189 Zymograms were performed to detect the cysteine desulfhydrase and homocysteine g-
190 lyase activities. Native protein crude extracts (40 and 100 µg, respectively) were run on a
191 non-denaturing protein gel (12% polyacrylamide in Tris-Glycine buffer). After
192 electrophoresis, the gel was incubated at 37°C for one to four hours in a Tris solution (50
193 mM Tris-HCl (pH 7.4), 10 mM MgCl₂, 0.5 mM Pb(NO₃)₂ and 5 mM DTT) with 0.4 mM
194 pyridoxal-5-phosphate (PLP) containing either 10 mM L-cysteine or 10 mM homocysteine
195 as previously described (32). H₂S formed by the cysteine desulfhydrase or homocysteine
196 γ-lyase activity precipitates as insoluble PbS.

197 **Construction of *C. difficile* mutants**

198 The ClosTron gene-knockout system (39) was used to inactivate genes encoding Fur
199 (*CD1287*), SigL (*CD3176*), CysK (*CD1594*) and a TCS-sensor histidine kinase (*CD2602*), as
200 well as several regulators of unknown function (*CD2065*, *CD0278* and *CD2023*; Table 1).
201 As described in Fig. S1, primers were designed to retarget the group-II intron of
202 pMTL007 to these genes (Table S1) and were used to generate a 353-bp DNA fragment
203 by overlap PCR according to the manufacturer's instructions. These PCR products were
204 cloned into the *Hind*III and *Bsr*GI restriction sites of the pMTL007 and were verified by
205 DNA sequencing using the pMTL007-F and pMTL007-R primers (Table S1). The derived
206 pMTL007 plasmids were transformed into *E. coli* strain HB101 (RP4) and transferred by
207 conjugation into the *C. difficile* strain 630Δ*erm*. *C. difficile* transconjugants were selected

208 by sub-culture on BHI agar containing thiamphenicol (15 µg/ml), and the integration of
209 the group-II intron RNA into genes was induced and selected by plating onto BHI agar
210 containing erythromycin (2.5 µg/ml). The chromosomal DNA of the transconjugants was
211 extracted using the InstaGene Kit (BioRad), and PCR using the primers ErmRAM-F and
212 ErmRAM-R (Table S1) was used to confirm the erythromycin-resistant phenotype due to
213 the splicing of the group-I intron from the group-II intron following integration (Fig.
214 S1A). The insertion of the group-II intron into target genes was verified by Southern blot
215 (Fig. S1C) and by PCRs (Fig. S1B) with primers flanking the 5' ends of genes (Table S1)
216 and EBSu primer. To knock down *maly* (*CD3029*) expression, a DNA fragment
217 comprising the 5' untranslated region (UTR) and the beginning of the *CD3029* open
218 reading frame (-38 to +154 from the ATG start codon) was amplified by PCR and cloned
219 between the *XhoI* and *BamHI* sites of the pRPF185 vector (36) to generate pDIA6456
220 expressing the 5' end of *maly* in the antisense orientation under the control of the ATc-
221 inducible *P_{tet}* promoter. This plasmid was transferred by conjugation into *C. difficile*
222 strain 630Δ*erm*. To complement the *sigL* mutant, the *sigL* gene and its promoter (-193 to
223 +1380 from the ATG start codon) were amplified by PCR using the appropriate primers
224 (Table S1). The PCR fragment was cloned into the *XhoI* and *BamHI* sites of pMTL84121
225 (40) to generate plasmid pDIA6309. This plasmid was transferred by conjugation into
226 the *C. difficile sigL* mutant (CDIP217), yielding strain CDIP342.

227 All experiments conducted with the mutants were standardized versus the wild type for
228 the culture growth (OD₆₀₀) and the protein concentration of the samples or by using a
229 reference gene for the qRT-PCR assays.

230 RNA isolation and quantitative real-time PCR

231 *C. difficile* strains were grown in PY or PYC for 10 h. Total RNA extraction was performed
232 using the FastRNA Pro Blue kit and a Fastprep apparatus according to the manufacturer's
233 instructions (MP Biomedicals) as previously described (13). To synthesize cDNA, 1 µg of
234 total RNA was heated at 70°C for 10 min in the presence of 1 µg of hexamer
235 oligonucleotide primers (pdN₆, Roche). RNAs were then reverse transcribed for 2 h at
236 37°C using AMV Reverse transcriptase (RT) (Promega), 20 mM dNTPs and 40 U of RNasin
237 (Promega). Reverse transcriptase was inactivated by heating at 85°C for 5 min. Real-time
238 quantitative RT-PCR was performed in a 20-ml reaction volume containing 20 ng of
239 cDNAs, FastStart SYBR Green Master mix (ROX, Roche) and 200 nM of gene-specific

240 primers (Table S1). Amplification and detection were performed as previously described
241 (13). The quantity of each cDNA was normalized to the quantity of the cDNA of the DNA
242 *polIII* gene (CD1305). The relative change in gene expression was recorded as the ratio to
243 normalized target concentrations ($\Delta\Delta Ct$) (41). Shapiro-Wilk test was performed to test
244 the normality of the replicates for each condition (Table S3). When population of the two
245 conditions was normally distributed a t-test was used, otherwise we used a Mann-
246 Whitney test as indicated in the legend of figures. A p-value ≤ 0.05 was considered
247 significant.

248 **Microarray design for the *C. difficile* genome, DNA-array hybridization and data** 249 **analysis.**

250 The microarray of the *C. difficile* strain 630 genome was designed as previously described
251 (15) (GEO database accession number [GPL10556](https://www.ncbi.nlm.nih.gov/geo/query/acc.cgi?acc=GPL10556)). The transcriptome was performed
252 with four different RNA preparations and a dye-swap method. First, 10 μg of total RNA
253 was reverse transcribed in cDNA using the SuperScript Indirect cDNA labeling system kit
254 (Invitrogen) and Cy3 or Cy5 fluorescent dye (GE Healthcare) according to the
255 manufacturer's recommendations. Labeled DNA hybridization to microarrays and array
256 scanning were performed as previously described (15). The complete experimental data
257 set was deposited in the GEO database with accession number GSE22423. All slides were
258 analyzed using the R and limma software (Linear Model for Microarray Data) from the
259 Bioconductor project (www.bioconductor.org). For each slide, we corrected for
260 background with the 'normexp' method (42), which resulted in strictly positive values
261 and reduced variability in the log ratios for genes with low hybridization signal levels.
262 Then, we normalized each slide by the 'loess' method (43). To test for differential
263 expression, we used Bayesian adjusted t-statistics and performed the multiple-testing
264 correction of Benjamini & Hochberg based on the false discovery rate (FDR) (44). A gene
265 was considered to be differentially expressed when the p-value was < 0.05 .

266 **Raw sequences analysis**

267 The presence of the TCS locus (CD2602-26021) was inferred from raw sequences of 2424
268 published strains (Sequence Read Archive (SRA) accession numbers: PRJEB2039,
269 PRJEB4556, PRJEB3010, PRJEB190-216, PRJEB6600-2, PRJEB6575). For that purpose, we
270 mapped the sequencing reads of each strain onto the nucleotide sequence of the TCS locus

271 using Bowtie (1). A strain was considered to contain the TCS locus when the coverage was
272 above 80%.

273

274 **Results & discussion**

275

276 **Cysteine-dependent repression of PaLoc genes**

277 It has been shown that toxin synthesis is repressed by cysteine in the high-toxin-level-
278 producing strain VPI10463 (12). To determine whether the effect of cysteine on toxin
279 synthesis is strain-dependent, we measured the effect of cysteine on toxin production in
280 several *C. difficile* backgrounds (Table 1), such as strains 630 Δ *erm* and M7404 (a
281 NAP1/027 epidemic strain), as well as a M7404-derivative strain carrying a wild-type
282 copy of the *tcdC* gene on the pDLL17 plasmid (2); VPI10463 was used as a control. All of
283 the strains grew similarly in PY with or without cysteine. Cell crude extracts were
284 obtained from these four strains after 10 h of growth in PY or PYC, and toxin production
285 was assayed by Vero cell cytotoxicity assays, which predominantly assess TcdB, and
286 protein dot-blot analysis using a specific antibody raised against TcdA. Cytotoxic activity
287 was lower in cells grown in the presence of cysteine (Fig. 2A) compared to cells grown
288 without cysteine, with 25- to 125-fold decreased cytotoxicity for strains 630 Δ *erm*, M7404
289 and M7404 + pDLL17-*tcdC* and 16000-fold decreased cytotoxicity for strain VPI10463.
290 Moreover, TcdA accumulation was strongly reduced in the presence of cysteine in all of
291 the strains tested (Fig. 2B). These results suggest that cysteine-dependent repression of
292 toxin production is conserved among the *C. difficile* strains. Cysteine repressed toxin
293 synthesis in both the epidemic 027 strain M7404, which does not express functional TcdC,
294 and in its derivative strain that contains a wild-type *tcdC* gene (2). Thus, the effect of
295 cysteine on toxin production is not mediated by TcdC.

296 To determine whether the effect of cysteine on toxin production occurred at the
297 transcriptional level, we performed qRT-PCR experiments for the *tcdA*, *tcdB* and *tcdR*
298 genes using strain 630 Δ *erm* (Fig. 2C). After 10 h of growth, transcript level of *tcdA* and
299 *tcdB* decreased 18- and 17-fold, respectively, in the presence of cysteine. We also
300 observed that the expression of the *tcdR* gene encoding the alternative sigma factor
301 required for toxin-gene transcription decreased 40-fold when cysteine was added (Fig.
302 2C). These data are in agreement with the results obtained by Karlsson et al. (11),

303 suggesting that toxin-gene transcription is repressed by cysteine through negative
304 regulation of *tcdR*.

305 **Reconstruction of sulfur metabolism in *C. difficile***

306 An understanding of sulfur metabolism was a prerequisite to elucidating how cysteine
307 negatively regulates toxin production. To reconstitute the sulfur-metabolism pathways,
308 we first searched for all of the gene homologs to the genes involved in sulfur-assimilation
309 pathways in other firmicutes (30) in the complete genome sequence of the reference *C.*
310 *difficile* strain 630 (45) (Fig. 3). All genes identified are conserved in the VPI10463 and
311 NAP1/027 epidemic strains (Table S4). Then, to support the metabolic reconstruction
312 and to obtain new insights about the physiology of *C. difficile*, we tested the ability of
313 strain 630 Δ *erm* to grow in minimal media with different sulfur sources (Table 2).

314 Strain 630 Δ *erm* cannot grow when sulfate is the only sulfur source (Table 2). This finding
315 is consistent with the absence of genes involved in the first steps of the sulfate-
316 assimilation pathway leading to sulfite (Fig. 1). By contrast, strain 630 Δ *erm* was able to
317 grow in the presence of sulfide or thiosulfate (Table 2), indicating that *C. difficile* can
318 synthesize cysteine from these compounds, probably through the CysE/CysK thiolation
319 pathway (Fig. 3). Cysteine can also be produced from glutathione, a sulfur source utilized
320 by strain 630 Δ *erm* (Table 2). PepT and PepA are probably involved in the degradation of
321 glutathione to form cysteine (Fig. 3). However, the pathway of glutathione synthesis from
322 cysteine that is found in *C. perfringens* (20) is absent in *C. difficile*. Strain 630 Δ *erm* can also
323 grow with cysteine as the sole sulfur source, indicating that methionine is efficiently
324 produced from this compound. As shown in Fig. 3, methionine is synthesized from
325 homocysteine, likely through the cobalamine-dependent methionine synthase MethH. The
326 two main pathways of homocysteine production in bacteria are transsulfuration and
327 thiolation (Fig. 1) (30). Both pathways involve PLP-dependent enzymes: transsulfuration
328 requires a cystathionine γ -synthase and a cystathionine β -lyase, while thiolation requires
329 an *O*-acetyl-homoserine (OAH)-thiol-lyase (Fig. 1). In the genome of strain 630, three PLP-
330 dependent enzymes were identified by their similarities: MetY, MalY and MdeA (46). MetY
331 contains an amino-acid insertion specific to OAH-thiol-lyases, MalY is a cystathionine β -
332 lyase of the PatB/MalY family (32), and MdeA is a probable methionine γ -lyase. However,
333 no cystathionine γ -synthase is present in *C. difficile*, suggesting that a functional

334 transsulfuration pathway is absent and that *C. difficile* synthesizes both methionine and
335 cysteine by thiolation pathways.

336 **Homocysteine and Cysteine degradation**

337 Strain 630 Δ *erm* can grow in the presence of homocysteine and, to a lesser extent, in the
338 presence of cystathionine, but cannot use methionine as the sole sulfur source (Table 2).
339 The ability to use homocysteine is surprising because the reverse transsulfuration
340 pathway, which involves a cystathionine β -synthase and a cystathionine γ -lyase (Fig. 1), is
341 absent in *C. difficile* (31, 47). Growth in the presence of homocysteine could be explained
342 by the existence of a homocysteine γ -lyase, allowing the production of H₂S from
343 homocysteine and its possible conversion into cysteine (Fig. 3). Using lead-acetate paper,
344 we detected the production of H₂S during the growth of strain 630 Δ *erm* in PY plus
345 homocysteine (PYHC), but not in PY alone (Fig. 4A). When we performed a zymogram
346 using homocysteine as a substrate, we detected a single band in crude extracts of strain
347 630 Δ *erm* grown in PY, PYC and PYHC (Fig. 4B), suggesting that homocysteine γ -lyase
348 activity is induced in all of the growth conditions used. Among the PLP-dependent
349 enzymes encoded by the *C. difficile* genome, MdeA shares significant similarities with the
350 methionine γ -lyases of *Citrobacter freundii* (48) and of *Brevibacterium linens*.
351 Interestingly, the methionine γ -lyase of *B. linens* also has homocysteine γ -lyase activity
352 (49), making MdeA a probable candidate for the production of H₂S from homocysteine
353 and the degradation of methionine to form methanethiol in *C. difficile* (Fig. 3), as
354 previously proposed (50).

355 In bacteria, cysteine is usually catabolized by cysteine desulhydrases (32), producing
356 H₂S, pyruvate and ammonia (Fig. 1). We detected high production of H₂S during the
357 growth of strain 630 Δ *erm* in PYC (Fig. 4A). Indeed, the quantification of H₂S showed a 20-
358 to 30-fold increase of H₂S production when cysteine was added to the medium (Fig. 4C).
359 This result clearly indicated that cysteine is efficiently degraded in *C. difficile*. To detect
360 the cysteine desulhydrase activities, we performed a zymogram using L-cysteine as
361 substrate. We detected two bands (α and γ) in the crude extract of strain 630 Δ *erm* grown
362 in PY (Fig. 4D, lane 1). Interestingly, when strain 630 Δ *erm* was grown in PYC, we detected
363 an additional band (β), indicating that synthesis of this desulhydrase enzyme was
364 induced by cysteine (Fig. 4D, lane 2). In *B. subtilis*, PatB/MalY- and CysK-type enzymes
365 have cysteine desulhydrase activities (32). To determine whether CysK of *C. difficile* is a

366 cysteine desulfhydrase, we inactivated the *cysK* gene in strain 630 Δ *erm* using the
367 Clostron system (Fig. S1). The zymogram profile obtained with the *cysK* mutant strain
368 grown in PYC is similar to that obtained with the 630 Δ *erm* strain (Fig. 4D, lane 3). This
369 finding suggests that CysK is not a major cysteine desulfhydrase in *C. difficile* under the
370 conditions tested, although we cannot exclude a role for CysK in cysteine degradation. We
371 failed to inactivate the gene encoding the PatB/MalY enzyme, probably because of its
372 essentiality for *C. difficile* (51). Thus, to evaluate whether PatB/MalY is a cysteine
373 desulfhydrase, we constructed a PatB/MalY-depleted strain using an antisense strategy
374 (36, 52). Compared to the strain carrying the control plasmid (Fig. 4D lane 5), the
375 PatB/MalY-depleted strain (Fig. 4D lane 6) displayed a decreased intensity of the α band,
376 suggesting that MalY has cysteine desulfhydrase activity. However, the enzymes with
377 cysteine desulfhydrase activity corresponding to γ and β bands on the zymogram (Fig.
378 4D) remain to be identified.

379 Finally, we demonstrated that both homocysteine and cysteine are actively catabolized by
380 *C. difficile*. Interestingly, it has recently been shown that when *C. difficile* grows in minimal
381 media with casminoacids, cysteine is consumed immediately and sulfide is produced (53).
382 This finding is in complete agreement with our results. Thus, we propose that sulfide is a
383 central compound of sulfur metabolism in *C. difficile*, as it is the direct precursor of both
384 methionine and cysteine, as well as the major degradation product of the sulfur-
385 containing amino acids homocysteine and cysteine (Fig. 3).

386 **Global analysis of genes expression in response to cysteine**

387 To determine the global impact of cysteine on gene expression and to elucidate the
388 mechanism of cysteine-dependent repression of toxin production, we performed a
389 comparative transcriptional analysis of strain 630 Δ *erm* grown in PY or PYC at the onset of
390 stationary phase (10 h). In the presence of 10 mM cysteine, 6 % of the genome (201
391 genes) was differentially expressed with a fold change ≥ 2 (Table S2). Among these genes,
392 120 and 81 were up- and down-regulated, respectively. The major expression changes
393 were seen in genes encoding cell-surface-associated proteins and proteins involved in
394 sulfur, amino-acid, carbon and energy metabolism as well as in iron uptake (Table S2).
395 The transcriptomic analysis confirmed that toxin-gene expression decreased in the
396 presence of cysteine. In addition, exposure of *C. difficile* to high cysteine concentrations
397 strongly induced the expression of genes encoding heat-shock proteins belonging to both

398 Class I (HrcA-dependent), such as the *groESL* and *hrcA* operons, and Class III (CtsR-
399 dependent), such as the *ctsR* and the *clpB* operons. We validated the transcriptomic
400 analysis by performing qRT-PCR with a selection of 12 representative genes. The results
401 confirmed the microarray data (Table S2).

402 **Regulation of genes involved in sulfur metabolism and in thiol protection by** 403 **cysteine**

404 As expected, the expression of genes related to sulfur metabolism, including transporters
405 of amino acids, was controlled by cysteine. The *metQ₁* gene encoding the methionine-
406 binding protein of an ABC transporter (54, 55) (Fig. 3) was less strongly expressed in PYC.
407 This gene is probably regulated by a S-box riboswitch in the promoter region of the
408 *metN₁Q₁* operon, like most of the genes required for methionine uptake (Fig. 3) (55, 56).
409 The ABC transporter system composed of CD2177, CD2176, CD2175, CD2174 and
410 CD2172 is likely involved in the uptake of cystine and/or cysteine in *C. difficile* (Fig. 3).
411 CD2177 and CD2174 share similarities with the cystine-binding proteins of *E. coli* and *B.*
412 *subtilis* (57), while CD2176 and CD2175 are similar to the L-cystine permeases of *E. coli*
413 and *B. subtilis*. The expression of all of the genes encoding this ABC transporter decreased
414 2.5- to 4-fold in PYC, as is usually observed for cysteine/cystine transporters. By contrast,
415 the expression of the *ssuA₂* and *ssuC₂* genes, which encode proteins sharing similarities
416 with sulfonate ABC transporters, increased in the presence of cysteine (Fig. 3).

417 The expression of CysK encoding the OAS-thiol-lyase and CysE, the serine acetyl-
418 transferase was induced 40- to 50-fold in the presence of cysteine (Fig. 3 and Table S2).
419 The up-regulation of *cysKE* expression in PYC is surprising because CysK and CysE, which
420 are required for cysteine biosynthesis, are usually induced during cysteine limitation, as
421 previously observed in *C. perfringens*, *B. subtilis*, *E. coli* and Salmonella (20, 30, 34).
422 However, in the presence of high cysteine concentrations, CysK contributes to cysteine
423 degradation rather than cysteine synthesis (58). Under these conditions, CysE activity is
424 inhibited by feedback, as established in several bacteria and plants (38, 59). Nonetheless,
425 the role of CysK in cysteine metabolism remains to be clarified.

426 Finally, we observed that genes involved in thiol protection were induced in the presence
427 of cysteine (Table S2). They encode two thioredoxins (*CD1690* and *CD2355*), a thioredoxin
428 reductase (*CD1691*) and a thiol peroxidase (*CD1822*). The induction of genes involved in
429 thiol protection and in the stress response suggests that cysteine or its derivative

430 products (e.g., H₂S) stress *C. difficile*. However, the addition of 10 mM cysteine to the PY
431 medium did not affect *C. difficile* growth and cell viability (data not shown) while this
432 amino acid is toxic in other bacteria, such as *E. coli* and *B. subtilis* ((60); I. Martin-
433 Verstraete, unpublished results). The expression of the stress-responsive genes in
434 relation to the absence of cysteine toxicity in *C. difficile* may be the result of an adaptation
435 to an anaerobic lifestyle.

436 **Induction of *fur* and Fur-regulated genes in the presence of cysteine**

437 The ferric uptake regulator (Fur) protein is an iron-response repressor that controls the
438 expression of genes involved in iron transport in bacteria (61, 62). The CD1287 protein
439 shares 48 % identity with the Fur protein of *B. subtilis*. To demonstrate that CD1287
440 corresponds to Fur, we constructed a *CD1287* mutant strain using the ClosTron system
441 (Fig. S1). Then, we tested the effect of *CD1287* disruption on the level of transcription of
442 the *feoB1* and *fhuD* genes by qRT-PCR. In *B. subtilis*, FeoB1 and FhuD participate in ferrous
443 iron and ferrichrome uptake, respectively (61, 63). We showed that the addition of 200
444 mM of dipyriddy, a ferrous iron chelator, to the growth medium increased the transcript
445 level of the *CD1287*, *fhuD* and *feoB1* genes and that transcription of *feoB1* and *fhuD*
446 increased 3500- and 45-fold, respectively, in the *CD1287* mutant compared to the wild-
447 type strain (data not shown). These results strongly indicate that CD1287 is the Fur
448 repressor in *C. difficile*, as recently demonstrated (64).

449 From our global transcriptomic analysis, we found that the presence of cysteine in the
450 medium induced the Fur-regulon, including *fur* and genes encoding transporters of
451 ferrous iron and ferrichrome (Table 3). Using the Fur-binding site of *B. subtilis* (61), we
452 detected a potential Fur box upstream of approximately 20 genes that are differentially
453 expressed in PYC, including *fur*, *feoB1*, *cysK* and *fhuD*, as well as genes encoding proteins
454 of unknown function, such as *CD2992*, *CD1485*, *CD2499* and *CD2881* (Table 3). The
455 consensus Fur box for *C. difficile* (Fig. 5A), deduced from the putative Fur-binding motifs
456 present in the regulatory region of these genes, is highly similar to that defined by Ho et
457 al. (64). We then tested the effect of cysteine on the transcription of some of these Fur
458 targets by qRT-PCR in both 630 Δ *erm* and a *fur* mutant strain. In the presence of cysteine,
459 the transcript level of *fur*, *feoB1*, *cysK*, *fhuD* and *CD2992* genes increased 3.2-, 750-, 56-,
460 12- and 10-fold, respectively, in strain 630 Δ *erm* (Fig. 5B), a result consistent with the
461 transcriptome data (Table 3). The cysteine-dependent up-regulation of *feoB1*, *fhuD* and

462 *CD2992* was abolished in the *fur* mutant, indicating that the effect of cysteine is mediated
463 by the Fur repressor. Interestingly, the induction of *cysK* transcription by cysteine was not
464 completely abolished in the *fur* mutant and was only five-fold lower than it was in strain
465 630 Δ *erm* (Fig. 5B). In addition, in the absence of cysteine, the transcript level of *cysK* was
466 4.5-fold higher in the *fur* mutant than in strain 630 Δ *erm* (data not shown). As a Fur box is
467 located in the promoter region of the *cysK* gene, the regulation of *cysK* by cysteine is
468 complex, involving both direct regulation by the Fur repressor and control by a still-
469 uncharacterized regulator. While very few data concerning the control of *cysK* expression
470 by Fur are available (65), the cysteine-dependent regulation of CysK synthesis in *C.*
471 *difficile* seems to be atypical.

472 The induction of the Fur regulon by cysteine suggests that the presence of cysteine in the
473 growth medium mimics the conditions of iron depletion. A black precipitate appears
474 when strain 630 Δ *erm* is grown in PYC (Fig. 5C). This finding is consistent with the
475 production of high levels of H₂S via cysteine degradation by cysteine desulhydrases (Fig.
476 4C), which probably leads to the formation of this black deposit from iron-sulfide
477 precipitation. This phenomenon is often described in anaerobic waste-collection systems
478 (66). Therefore, iron depletion due to the precipitation of iron in the presence of excess
479 sulfide can explain the induction of the Fur-regulated genes.

480 **Regulation by cysteine of carbon and energy metabolism**

481 The ability of *C. difficile* to use a wide range of carbohydrates might be important during
482 infection. Accordingly, Antunes et al. (13) demonstrated the existence of links between
483 carbon metabolism and toxin production. The addition of cysteine to the medium
484 increased the expression of several genes of carbon metabolism, including genes encoding
485 phosphotransferase systems (PTS) and genes encoding enzymes involved in the second
486 part of glycolysis (Fig. 6A and-Table S2).

487 The expression of genes involved in the fermentation pathways of *C. difficile* was also
488 modulated by the presence of cysteine (Fig. 6A). Thus, the expression of *ldh* and *buk*,
489 which encode lactate dehydrogenase and one butyrate kinase, respectively, decreased,
490 while the expression of genes encoding pyruvate formate lyases and an alcohol
491 dehydrogenase, increased in the presence of cysteine. Surprisingly, the *bcd2* operon,
492 which is involved in the production of butyryl-CoA from acetyl-CoA (Fig. 6A), was not
493 differentially expressed in the transcriptome analysis. However, when we tested the effect

494 of cysteine on the expression of the *bcd2* and *hbd2* genes by qRT-PCR, we showed that
495 their transcript levels decreased 5.5- and 6-fold in PYC compared to PY, respectively. This
496 result is in agreement with the results of a proteome analysis performed in strain
497 VPI10463 (12), showing that the production of enzymes involved in the conversion of
498 acetyl-CoA to butyryl-CoA (*Bcd2*, *Crt2* and *Hbd*) decreases when cells are grown in
499 presence of cysteine. To evaluate the impact of cysteine on fermentation pathways, we
500 quantified the end products of fermentation in strain 630 Δ *erm* grown over 48 h in PY or
501 PYC by gas-liquid chromatography. The amount of lactate and butyrate was reduced four-
502 and six-fold, respectively, in the presence of cysteine (Fig. S2) as observed in strain
503 VPI10463 (12). This result is consistent with the down-regulation of *ldh*, *buk* and *bcd2*
504 operon expression. After 48 h of growth, butyric acid production was high in PY, leading
505 to a final concentration of 5 mM compared to less than 1 mM in PYC (Fig. S2).
506 Interestingly, the addition of butyric acid to the growth medium enhances toxin
507 production in strain VPI10463 (12). Thus, the addition of cysteine to the medium may
508 indirectly control toxin production at least partly via its influence on butyric acid
509 production. However, the molecular mechanisms of the regulation of toxin synthesis in
510 response to butyric-acid availability remain to be determined.

511 **Control of amino-acid metabolism by cysteine**

512 To analyze the impact of cysteine on amino-acid metabolism, we compared the
513 transcriptome and the pools of amino acids obtained from strain 630 Δ *erm* grown in PY or
514 PYC. A total of 32 genes involved in peptide or amino-acid metabolism were differentially
515 expressed under these two conditions (Table S2), while the intracellular concentration of
516 leucine, tyrosine, alanine, valine, phenylalanine and glutamic acid was increased in the
517 presence of cysteine (Table 4). The expression of several genes involved in peptide
518 degradation (*CD0779*, *CD2613*, *CD2347*, *CD2173* and *CD0166*) and amino-acid uptake
519 (*CD2612*, *CD3092* and *CD0165*) was differentially regulated when cysteine was added to
520 the medium (Fig. 6A). In *C. difficile*, amino-acid catabolism by the Stickland reactions can
521 be a primary source of energy when bacteria are grown with amino acids as the sole
522 carbon and nitrogen sources (67). Stickland reactions couple the metabolism of a pair of
523 amino acids, of which one serves as the Stickland donor (alanine, valine, leucine or
524 isoleucine) and is oxidatively deaminated or decarboxylated to generate ATP and
525 reducing power (NADH), and the second serves as the Stickland acceptor (glycine,

526 proline, hydroxyproline or leucine) and is reduced or reductively deaminated,
527 regenerating NAD⁺ from NADH (Fig. 6B). The genes encoding the glycine reductase (*grd*)
528 and D-proline reductase (*prd*) operons, which are involved in the reduction of the
529 Stickland acceptors glycine and proline, were induced up to 10-fold in the presence of
530 cysteine (Fig. 6B and Table S2). Interestingly, the expression of *proC* (*CD3281*), which is
531 involved in the conversion of ornithine into proline, and of *CD2347*, which encodes a
532 peptidase sharing similarities with Xaa-Pro dipeptidases and potentially generates free
533 proline for use in the Stickland reactions (67), was also increased in the presence of
534 cysteine.

535 In strain 630Δ*erm* grown in the presence of cysteine, we observed a substantial
536 accumulation of alanine (Table 4), a by-product of cysteine catabolism. Indeed, cysteine is
537 first converted into pyruvate through cysteine desulfhydrases; pyruvate is then converted
538 into alanine by alanine aminotransferases (Fig. 6A). *CD2828*, which shares similarities
539 with an alanine aminotransferase characterized in *E. coli* (68), is a good candidate for this
540 activity. However, *CD2828* was repressed in PYC (Table S2). The negative control of
541 *CD2828* expression in the presence of a high intracellular concentration of alanine might
542 explain this down-regulation

543 Several genes involved in the biosynthesis of branched-chain amino acids (BCAAs) were
544 also repressed by cysteine (Fig. 6A and Table S2). The expression of *ilvD* involved in the
545 BCAAs synthesis from pyruvate and of the *leuABCD* operon, which is involved in synthesis
546 of leucine were down-regulated 5- to 10-fold in the presence of cysteine. Interestingly, the
547 transcription of *brnQ1*, which encodes a BCAA transporter (Fig. 6A), was also decreased in
548 PYC. A Tbox specific to leucine (Tbox_{Leu}) is present in the promoter region of the *leuABCD*
549 operon and of the *leuS* gene, indicating that these genes are probably induced during
550 leucine starvation via premature termination of transcription (56, 69). We note that *ilvD*,
551 *leuABCD* and *brnQ1* belong to the CodY regulon, which is involved in the adaptive
552 response to nutrient limitation (17). Thus, the increase in the concentration of valine and
553 leucine when cysteine is added (Table 4) might lead to the repression of genes involved in
554 BCAAs biosynthesis and uptake through their control by a Tbox_{Leu} or by CodY. In *B.*
555 *subtilis*, changes in the rate of endogenous isoleucine, leucine and valine synthesis
556 modulate the expression of CodY-regulated genes (70). In addition, for *Clostridium*
557 *sticklandii*, using amino acids as the carbon and energy sources, cysteine is one of the six

558 amino acids that is preferentially degraded, while valine, leucine and isoleucine are used
559 later, suggesting that certain amino acids regulate the metabolism of others (71). Cysteine
560 is also one of the three amino acids that are preferentially used by *C. difficile* (53). Our
561 results suggest that the presence of cysteine may delay the use of other amino acids, such
562 as BCAAs, which are known to act as co-repressors of CodY (17). Accordingly, we
563 observed that 31 CodY-regulated genes were repressed in strain 630 Δ *erm* when cysteine
564 was added (Table S2), suggesting that cysteine has an impact on CodY activity.

565 **Involvement of regulators in the cysteine-dependent repression of toxin** 566 **production**

567 Toxin expression may be under the control of a global regulator that is able to sense
568 cysteine availability. Interestingly, we showed that several genes encoding regulators are
569 regulated in response to cysteine availability. Indeed, *CD0278*, *CD1692*, *CD2023* and
570 *CD2065* were up- or down-regulated in the presence of cysteine (Table S2). Using the
571 ClosTron system, we inactivated *CD0278*, *CD2023* and *CD2065*, but we did not succeed in
572 disrupting *CD1692*. Compared to the wild-type strain, toxin-gene expression was similarly
573 repressed by cysteine in the *CD0278*, *CD2023* and *CD2065* mutants (data not shown).
574 However, we cannot exclude the possibility that a still-unidentified regulator intervenes
575 in this control. Alternatively, the effector of cysteine-dependent regulation might be a
576 cysteine by-product that is accumulated during growth in PYC. To discriminate between a
577 direct effect of cysteine and an indirect metabolic effect, we added 10 mM cysteine to the
578 growth medium for one hour at the onset of the stationary phase. Surprisingly, under this
579 condition limiting the catabolism of cysteine, we observed that the transcription of *tcdA*,
580 *tcdB* and *tcdR* was increased (Fig. S3), suggesting that cysteine down-regulates toxin
581 production through a product of cysteine degradation (see below). As changes in carbon
582 source and amino-acid availability were observed after the growth of *C. difficile* in the
583 presence of cysteine (Fig. S2 and Table 4), we wondered whether toxin synthesis could be
584 controlled by the global regulators CodY or CcpA, which are known to regulate toxin-gene
585 expression in response to the levels of the BCAAs and PTS sugars, respectively (13, 14,
586 18). However, we showed that toxin synthesis is similarly repressed by cysteine in the
587 *codY* or *ccpA*-mutant and wild-type strains (Fig. 7A), indicating that CodY and CcpA do not
588 mediate the control of toxin synthesis by cysteine.

589 The Fur regulator might also be responsible for the cysteine-dependent regulation of

590 toxin synthesis. Indeed, the expression of many virulence factors in pathogenic bacteria is
591 negatively regulated by Fur in response to iron availability (72). We showed that TcdA
592 production is repressed by cysteine in a *fur* mutant in the same manner as the wild-type
593 strain (Fig. 7B), indicating that Fur is not involved in the down-regulation of toxin
594 production in PYC. This result was in agreement with the absence of the toxin genes in the
595 Fur transcriptome, as recently defined by Ho et al. (64).

596 **The role of SigL in the cysteine-dependent repression of toxin production**

597 In *C. difficile* strain VPI10463, it has been proposed that several proteins induced under
598 toxin-producing conditions (PY) might be controlled by SigL (11). The *sigL* gene encodes a
599 sigma factor belonging to the SigL/RpoN/ σ^{54} family, which is known to play an important
600 role in metabolism, adaptation and virulence (73-77). To evaluate the role of SigL in the
601 cysteine-dependent regulation of toxin synthesis, we inactivated the *sigL* gene (Fig. S1).
602 When we compared the level of toxin produced between the *sigL* mutant and the wild-
603 type strain 630 Δ *erm* by dot-blot analysis, we first observed that TcdA was produced at
604 higher levels in the *sigL* mutant than in the wild-type strain when the cells were grown in
605 PY medium (Fig. 7B). This effect might be due to decreased competition between SigL and
606 the toxin-specific sigma factor TcdR for the core enzyme of the RNA polymerase, as
607 already proposed for SigH (15). Surprisingly, we observed similar levels of TcdA
608 production in the *sigL* mutant grown in PY and PYC (Fig. 7B). To determine whether SigL
609 regulates toxin synthesis at the transcriptional level, we tested the transcription of *tcdA*,
610 *tcdB* and *tcdR* genes in 630 Δ *erm* and *sigL* mutant strains grown in PYC by qRT-PCR. As
611 shown in Fig. 7C, the transcript level of *tcdA*, *tcdB* and *tcdR* was approximately 25 to 50-
612 fold higher in the *sigL* mutant compared to the wild-type strain in the presence of
613 cysteine. Moreover, complementation of the *sigL* mutant by a wild-type copy of *sigL*
614 partially restored the cysteine-dependent repression of TcdA production (Fig. 7B) and of
615 PaLoc-gene transcription (Fig. 7C). These results indicate that SigL mediates the cysteine-
616 dependent regulation of toxin-gene expression. However, using the well-conserved
617 consensus sequence of SigL-dependent promoters (78), we did not find a SigL-type
618 promoter upstream of *tcdA*, *tcdB* and *tcdR*, suggesting that SigL indirectly regulates the
619 PaLoc genes, probably in response to an increase in the by-products of cysteine
620 degradation. Indeed, using lead-acetate paper, we showed that the production of H₂S via
621 cysteine degradation was strongly reduced in the *sigL* mutant compared to strain

622 630 Δ *erm* (Fig. 8A) and was restored by complementation with pDIA6309. Interestingly,
623 according to the zymogram profile obtained with the *sigL* mutant, we showed that the
624 cysteine desulfhydrase activity of MalY (α band) significantly decreased (Fig. 4D lane 4).
625 In addition, the expression of *maly* was four-fold lower in a *sigL* mutant compared to the
626 wild-type strain (data not shown). This finding is in agreement with the role of SigL in the
627 control of cysteine degradation in *C. difficile*. As pyruvate is the first product of cysteine
628 degradation, we measured the extracellular concentration of pyruvate. We observed that
629 in strain 630 Δ *erm*, the pyruvate concentration increased more than two-fold when we
630 added cysteine to the medium. However, the level of pyruvate decreased eight-fold in the
631 *sigL* mutant compared to the wild-type strain (Fig. 8B). In addition, the *sigL* mutant strain
632 complemented with the wild-type copy of *sigL* had a extracellular pyruvate concentration
633 similar to that in strain 630 Δ *erm* (Fig. 8B).

634 **Involvement of pyruvate as a signal mediating toxin-gene repression in response to** 635 **cysteine**

636 The accumulation of H₂S or pyruvate resulting from cysteine degradation during growth
637 may be the signal modulating toxin production. To test this hypothesis, we added 10 mM
638 of either Na₂S or pyruvate to the PY medium when bacteria reached the stationary growth
639 phase and harvested the cells after one hour of exposure. The addition of pyruvate or
640 Na₂S decreased the transcription of *tcdA*, *tcdB* and *tcdR* (Fig. 9A). Interestingly, the effect
641 of pyruvate was not abolished when we performed a similar experiment in the *sigL*
642 mutant (Fig. S4). This finding confirms that cysteine-dependent regulation of toxin
643 production is mainly the consequence of the products of cysteine degradation. We also
644 tested the effect of the pyruvate by-products such as formate and acetate on Paloc-gene
645 transcription. The addition of 10 mM formate or acetate to the growing cell for one hour
646 did not affect the transcription of *tcdA*, *tcdB* and *tcdR* (Fig. 9B). Thus, we concluded that
647 pyruvate and probably sulfide are metabolic signals mediating the cysteine-dependent
648 repression of toxin production. As the down-regulation of toxin-gene expression in the
649 presence of cysteine (Fig. 2C) is more prominent than in the presence of pyruvate or
650 sulfide alone (Fig. 9A), it is possible that the cysteine by-products could have a combined
651 effect on toxin production.

652 **Identification of a TCS regulating toxin-gene expression in response to pyruvate**

653 Pyruvate is a central metabolite of bacteria, and its cellular concentration is tightly
654 controlled. In a broad range of bacteria, including *E. coli* and *Bacillus licheniformis*,
655 pyruvate is excreted into the medium at the end of the exponential growth phase under
656 the conditions of overflow metabolism. This compound is further taken up and
657 metabolized (79, 80). In *E. coli*, the two-component system (TCS) YpdA/YpdB, which is also
658 present in *B. licheniformis* (81), reacts predominantly to the presence of exogenous
659 pyruvate and induces the expression of *yhjX*, which encodes a transporter of the major
660 facilitator superfamily (79). The YpdA/YpdB system probably contributes to nutrient
661 scavenging before entry into stationary phase. In the genome of all of the *C. difficile* strains
662 sequenced, we found a TCS (CD2602/CD2601) that is highly similar to YpdA/YpdB.
663 Importantly, the transmembrane-receptor domain of CD2602 shares 53% identity and
664 79% similarity with that of the histidine kinase YpdA, suggesting a common signal for
665 these kinases. To determine whether CD2602-CD2601 is involved in the regulation of
666 toxin-gene expression in response to the level of exogenous pyruvate, we inactivated the
667 *CD2602* gene in strain 630 Δ *erm* (Fig. S1). Then, we tested the effect of pyruvate on *tcdA*,
668 *tcdB* and *tcdR* transcription in the *CD2602* mutant. The temporary addition of pyruvate
669 during the growth of the *CD2602* mutant had a less pronounced effect on toxin-gene
670 transcription than it had in the wild-type strain (Fig. 9C). This result suggests that the
671 transcriptional regulation of *tcdA*, *tcdB* and *tcdR* in response to pyruvate availability is, at
672 least in part, mediated by the TCS CD2602-CD2601.

673 **Conclusion**

674 Addition of cysteine to PY medium leads to dramatic changes in the pattern of expression
675 of *C. difficile* genes involved in several processes, including sulfur and iron metabolism,
676 fermentation and the stress response. These effects on gene transcription are probably
677 related to modifications of the metabolite pools, as we showed for the repression of toxin
678 production by metabolic changes due to cysteine degradation and transcriptional control
679 by cysteine through a still-uncharacterized regulator. We identified SigL as a major
680 regulator of cysteine-dependent repression of *C. difficile* toxin production. We found that
681 the level of H₂S and pyruvate resulting from cysteine degradation by cysteine
682 desulfhydrases (32) was decreased in a *sigL* mutant, which no longer repressed toxin
683 genes in the presence of cysteine. A similar regulation of toxin production through the
684 metabolic conversion of cysteine to sulfate and pyruvate has been observed in *B. pertussis*

685 (21). SigL also seems to play an important role in the control of pyruvate metabolism in *L.*
686 *monocytogenes* (82), as observed in *C. difficile* with a drop in the pyruvate concentration
687 in the *sigL* mutant. Among the cysteine by-products produced in *C. difficile*, we
688 demonstrated that the addition of pyruvate or H₂S to PY is sufficient to repress toxin-gene
689 expression, suggesting that pyruvate and H₂S, rather than cysteine, must be metabolic
690 signals regulating toxin production. Interestingly, when strain 630Δ*erm* grows in the
691 presence of cysteine, genes involved in the synthesis of pyruvate from glucose or cysteine
692 are up-regulated, while genes required for pyruvate dissimilation leading to butyrate (*buk*
693 operon) and lactate (*ldh*) production or involved in the biosynthesis of amino acids or
694 fatty acids from pyruvate and acetyl-CoA, respectively, are down-regulated (Fig. 6). This
695 change leads to the accumulation of pyruvate in the extracellular medium (Fig7B), where
696 it is probably sensed by the membrane-associated kinase CD2602. Thus, in response to
697 pyruvate, the response regulator CD2601 might negatively control toxin-gene expression,
698 either directly or indirectly. Conversely, butyrate, which is known to positively regulate
699 toxin expression (12), is found at a lower concentration in the extracellular medium (Fig.
700 S2), which no longer stimulates toxin synthesis. Recently, it has been shown that *C.*
701 *difficile* can grow in all parts of the intestinal tract of a mouse model, while toxins are only
702 produced in the caecum and colon (83). Thus, according to the metabolites present in the
703 small intestine and in the colon, toxin genes might be differentially expressed in the gut.
704 Accordingly, formate and acetate (directly obtained from pyruvate) predominate in the
705 small intestine, while the levels of propionate and butyrate are higher in the colon (84).
706 Such a control has been described in *Salmonella typhimurium*; formate acts as a diffusible
707 signal to induce the expression of invasion genes in the small intestine, the site that is
708 preferentially colonized by this enteropathogen, while butyrate is present at higher
709 concentration in the colon and repress these genes (85, 86). It is tempting to speculate
710 that the high level of pyruvate in the small intestine represses the expression of *C. difficile*
711 toxin genes, while butyrate mainly present in the colon induces toxin synthesis. Further
712 biochemical studies will be necessary to characterize the signal-transduction pathway of
713 the CD2602-CD2601 TCS. Thus, the ability of *C. difficile* to monitor the pyruvate level to
714 adapt its physiology, metabolism and virulence might be crucial to the success of a CDI.

715

716

717 **Acknowledgments**

718 This work was supported by funding from the “Institut Pasteur”. M. Dancer-Thibonnier
 719 and T. Dubois are post-doctoral fellows from the PTR program funded by the Institut
 720 Pasteur (PTR256) and the French region Ile-de-France (DIM-Malinf), respectively. The
 721 authors thank Dr. Philippe Bouvet for his help with the CPG analysis and Dr. Roselyne
 722 Garnotel and Sophie Roulin for the intracellular amino-acid content assays.

723

724 **References**

725

- 726 1. **Freeman J, Bauer MP, Baines SD, Corver J, Fawley WN, Goorhuis B, Kuijper**
 727 **EJ, Wilcox MH.** 2010. The changing epidemiology of *Clostridium difficile*
 728 infections. *Clin Microbiol Rev* **23**:529-549.
- 729 2. **Carter GP, Douce GR, Govind R, Howarth PM, Mackin KE, Spencer J, Buckley**
 730 **AM, Antunes A, Kotsanas D, Jenkin GA, Dupuy B, Rood JI, Lyras D.** 2011. The
 731 anti-sigma factor TcdC modulates hypervirulence in an epidemic BI/NAP1/027
 732 clinical isolate of *Clostridium difficile*. *PLoS Pathog* **7**:e1002317.
- 733 3. **Mani N, Dupuy B.** 2001. Regulation of toxin synthesis in *Clostridium difficile* by
 734 an alternative RNA polymerase sigma factor. *Proceedings of the National*
 735 *Academy of Sciences of the United States of America* **98**:5844-5849.
- 736 4. **Matamouros S, England P, Dupuy B.** 2007. *Clostridium difficile* toxin expression
 737 is inhibited by the novel regulator TcdC. *Mol Microbiol* **64**:1274-1288.
- 738 5. **Govind R, Dupuy B.** 2012. Secretion of *Clostridium difficile* toxins A and B
 739 requires the holin-like protein TcdE. *PLoS Pathog* **8**:e1002727.
- 740 6. **Akerlund T, Svenungsson B, Lagergren A, Burman LG.** 2006. Correlation of
 741 disease severity with fecal toxin levels in patients with *Clostridium difficile*-
 742 associated diarrhea and distribution of PCR ribotypes and toxin yields in vitro of
 743 corresponding isolates. *J Clin Microbiol* **44**:353-358.
- 744 7. **Dupuy B, Sonenshein AL.** 1998. Regulated transcription of *Clostridium difficile*
 745 toxin genes. *Molecular Microbiology* **27**:107-120.
- 746 8. **Karlsson S, Dupuy B, Mukherjee K, Norin E, Burman LG, Akerlund T.** 2003.
 747 Expression of *Clostridium difficile* toxins A and B and their sigma factor TcdD is
 748 controlled by temperature. *Infection and Immunity* **71**:1784-1793.
- 749 9. **Deneve C, Delomenie C, Barc MC, Collignon A, Janoir C.** 2008. Antibiotics
 750 involved in *Clostridium difficile*-associated disease increase colonization factor
 751 gene expression. *J Med Microbiol* **57**:732-738.
- 752 10. **Bouillaut L, Self WT, Sonenshein AL.** 2013. Proline-dependent regulation of
 753 *Clostridium difficile* Stickland metabolism. *J Bacteriol* **195**:844-854.
- 754 11. **Karlsson S, Burman LG, Akerlund T.** 2008. Induction of toxins in *Clostridium*
 755 *difficile* is associated with dramatic changes of its metabolism. *Microbiology*
 756 **154**:3430-3436.
- 757 12. **Karlsson S, Lindberg A, Norin E, Burman LG, Akerlund T.** 2000. Toxins,
 758 Butyric Acid, and Other Short-Chain Fatty Acids Are Coordinately Expressed and
 759 Down-Regulated by Cysteine in *Clostridium difficile*. *Infection and Immunity*
 760 **68**:5881-5888.

- 761 13. **Antunes A, Martin-Verstraete I, Dupuy B.** 2011. CcpA mediated repression of
762 *Clostridium difficile* toxin gene expression. Mol Microbiol **in press**.
- 763 14. **Dineen SS, Villapakkam AC, Nordman JT, Sonenshein AL.** 2007. Repression of
764 *Clostridium difficile* toxin gene expression by CodY. Mol Microbiol **66**:206-219.
- 765 15. **Saujet L, Monot M, Dupuy B, Soutourina O, Martin-Verstraete I.** 2011. The key
766 sigma factor of transition phase, SigH, controls sporulation, metabolism and
767 virulence factor expression in *Clostridium difficile*. J Bacteriol doi:JB.00272-11
768 [pii]10.1128/JB.00272-11.
- 769 16. **Underwood S, Guan S, Vijayasubhash V, Baines SD, Graham L, Lewis RJ,
770 Wilcox MH, Stephenson K.** 2009. Characterization of the sporulation initiation
771 pathway of *Clostridium difficile* and its role in toxin production. J Bacteriol
772 **191**:7296-7305.
- 773 17. **Dineen SS, McBride SM, Sonenshein AL.** 2010. Integration of metabolism and
774 virulence by *Clostridium difficile* CodY. J Bacteriol **192**:5350-5362.
- 775 18. **Antunes A, Camiade E, Monot M, Courtois E, Barbut F, Sernova NV, Rodionov
776 DA, Martin-Verstraete I, Dupuy B.** 2012. Global transcriptional control by
777 glucose and carbon regulator CcpA in *Clostridium difficile*. Nucleic Acids Res
778 **40**:10701-10718.
- 779 19. **Theriot CM, Koenigsnecht MJ, Carlson PE, Jr., Hatton GE, Nelson AM, Li B,
780 Huffnagle GB, J ZL, Young VB.** 2014. Antibiotic-induced shifts in the mouse gut
781 microbiome and metabolome increase susceptibility to *Clostridium difficile*
782 infection. Nat Commun **5**:3114.
- 783 20. **Andre G, Haudecoeur E, Monot M, Ohtani K, Shimizu T, Dupuy B, Martin-
784 Verstraete I.** 2010. Global regulation of gene expression in response to cysteine
785 availability in *Clostridium perfringens*. BMC Microbiol **10**:234.
- 786 21. **Bogdan JA, Nazario-Larrieu J, Sarwar J, Alexander P, Blake MS.** 2001.
787 Bordetella pertussis autoregulates pertussis toxin production through the
788 metabolism of cysteine. Infect Immun **69**:6823-6830.
- 789 22. **Grifantini R, Bartolini E, Muzzi A, Draghi M, Frigimelica E, Berger J,
790 Randazzo F, Grandi G.** 2002. Gene expression profile in *Neisseria meningitidis*
791 and *Neisseria lactamica* upon host-cell contact: from basic research to vaccine
792 development. Ann NY Acad Sci **975**:202-216.
- 793 23. **Hatzios SK, Bertozzi CR.** 2011. The regulation of sulfur metabolism in
794 Mycobacterium tuberculosis. PLoS Pathog **7**:e1002036.
- 795 24. **Mendez J, Reimundo P, Perez-Pascual D, Navais R, Gomez E, Guijarro JA.**
796 2011. A novel cdsAB operon is involved in the uptake of L-cysteine and
797 participates in the pathogenesis of *Yersinia ruckeri*. J Bacteriol **193**:944-951.
- 798 25. **Shelver D, Rajagopal L, Harris TO, Rubens CE.** 2003. MtaR, a regulator of
799 methionine transport, is critical for survival of group B streptococcus in vivo. J
800 Bacteriol **185**:6592-6599.
- 801 26. **Xayarath B, Marquis H, Port GC, Freitag NE.** 2009. *Listeria monocytogenes*
802 CtaP is a multifunctional cysteine transport-associated protein required for
803 bacterial pathogenesis. Mol Microbiol **74**:956-973.
- 804 27. **Soutourina O, Dubrac S, Poupel O, Msadek T, Martin-Verstraete I.** 2010. The
805 pleiotropic CymR regulator of *Staphylococcus aureus* plays an important role in
806 virulence and stress response. PLoS Pathog **6**:e1000894.
- 807 28. **Masip L, Veeravalli K, Georgiou G.** 2006. The many faces of glutathione in
808 bacteria. Antioxid Redox Signal **8**:753-762.

- 809 29. **Zeller T, Klug G.** 2006. Thioredoxins in bacteria: functions in oxidative stress
810 response and regulation of thioredoxin genes. *Naturwissenschaften* **93**:259-266.
- 811 30. **Guédon E, Martin-Verstraete I.** 2007. Cysteine metabolism and its regulation in
812 bacteria, p 195-218. *In* Wendisch VF (ed), *Amino acid biosynthesis-pathways,*
813 *regulation and metabolic engineering.* Springer.
- 814 31. **Hullo MF, Auger S, Soutourina O, Barzu O, Yvon M, Danchin A, Martin-**
815 **Verstraete I.** 2007. Conversion of methionine to cysteine in *Bacillus subtilis* and
816 its regulation. *J Bacteriol* **189**:187-197.
- 817 32. **Auger S, Gomez MP, Danchin A, Martin-Verstraete I.** 2005. The PatB protein of
818 *Bacillus subtilis* is a C-S-lyase. *Biochimie* **87**:231-238.
- 819 33. **Gutierrez-Preciado A, Henkin TM, Grundy FJ, Yanofsky C, Merino E.** 2009.
820 Biochemical features and functional implications of the RNA-based T-box
821 regulatory mechanism. *Microbiol Mol Biol Rev* **73**:36-61.
- 822 34. **Even S, Burguière P, Auger S, Soutourina O, Danchin A, Martin-Verstraete I.**
823 2006. Global control of cysteine metabolism by CymR in *Bacillus subtilis*. *J*
824 *Bacteriol* **188**:2184-2197.
- 825 35. **Soutourina O, Poupel O, Coppee JY, Danchin A, Msadek T, Martin-Verstraete**
826 **I.** 2009. CymR, the master regulator of cysteine metabolism in *Staphylococcus*
827 *aureus*, controls host sulfur source utilization and plays a role in biofilm
828 formation. *Mol Microbiol* **73**:194-211.
- 829 36. **Fagan RP, Fairweather NF.** 2011. *Clostridium difficile* has two parallel and
830 essential Sec secretion systems. *J Biol Chem* **286**:27483-27493.
- 831 37. **Lopez del Castillo Lozano M, Tache R, Bonnarme P, Landaud S.** 2007.
832 Evaluation of a quantitative screening method for hydrogen sulfide production
833 by cheese-ripening microorganisms: the first step towards l-cysteine catabolism.
834 *J Microbiol Methods* **69**:70-77.
- 835 38. **Tanous C, Soutourina O, Raynal B, Hullo MF, Mervelet P, Gilles AM, Noirot P,**
836 **Danchin A, England P, Martin-Verstraete I.** 2008. The CymR Regulator in
837 Complex with the Enzyme CysK Controls Cysteine Metabolism in *Bacillus subtilis*.
838 *J Biol Chem* **283**:35551-35560.
- 839 39. **Heap JT, Pennington OJ, Cartman ST, Carter GP, Minton NP.** 2007. The
840 Clostron: A universal gene knock-out system for the genus *Clostridium*. *J*
841 *Microbiol Methods* **70**:452-464.
- 842 40. **Heap JT, Pennington OJ, Cartman ST, Minton NP.** 2009. A modular system for
843 *Clostridium* shuttle plasmids. *J Microbiol Methods* **78**:79-85.
- 844 41. **Livak KJ, Schmittgen TD.** 2001. Analysis of relative gene expression data using
845 real-time quantitative PCR and the 2^{(-Delta Delta C(T))} Method. *Methods*
846 **25**:402-408.
- 847 42. **Breitling R, Armengaud P, Amtmann A, Herzyk P.** 2004. Rank products: a
848 simple, yet powerful, new method to detect differentially regulated genes in
849 replicated microarray experiments. *FEBS Lett* **573**:83-92.
- 850 43. **Smyth GK, Speed T.** 2003. Normalization of cDNA microarray data. *Methods*
851 **31**:265-273.
- 852 44. **Benjamini Y, Hochberg Y.** 1995. Controlling the false discovery rate: a practical
853 and powerful approach to multiple testing. *J Roy Statist Soc Ser*:289--300.
- 854 45. **Sebahia M, Wren BW, Mullany P, Fairweather NF, Minton N, Stabler R,**
855 **Thomson NR, Roberts AP, Cerdeno-Tarraga AM, Wang H, Holden MT, Wright**
856 **A, Churcher C, Quail MA, Baker S, Bason N, Brooks K, Chillingworth T,**
857 **Cronin A, Davis P, Dowd L, Fraser A, Feltwell T, Hance Z, Holroyd S, Jagels K,**

- 858 **Moule S, Mungall K, Price C, Rabbinowitsch E, Sharp S, Simmonds M, Stevens**
 859 **K, Unwin L, Whithead S, Dupuy B, Dougan G, Barrell B, Parkhill J.** 2006. The
 860 multidrug-resistant human pathogen *Clostridium difficile* has a highly mobile,
 861 mosaic genome. *Nat Genet* **38**:779-786.
- 862 46. **Mehta PK, Christen P.** 2000. The molecular evolution of pyridoxal-5'-phosphate-
 863 dependent enzymes. *Adv Enzymol Relat Areas Mol Biol* **74**:129-184.
- 864 47. **Andre G, Even S, Putzer H, Burguiere P, Croux C, Danchin A, Martin-**
 865 **Verstraete I, Soutourina O.** 2008. S-box and T-box riboswitches and antisense
 866 RNA control a sulfur metabolic operon of *Clostridium acetobutylicum*. *Nucleic*
 867 *Acids Res* **36**:5955-5969.
- 868 48. **Manukhov IV, Mamaeva DV, Rastorguev SM, Faleev NG, Morozova EA,**
 869 **Demidkina TV, Zavilgelsky GB.** 2005. A gene encoding L-methionine gamma-
 870 lyase is present in Enterobacteriaceae family genomes: identification and
 871 characterization of *Citrobacter freundii* L-methionine gamma-lyase. *J Bacteriol*
 872 **187**:3889-3893.
- 873 49. **Dias B, Weimer B.** 1998. Purification and characterization of L-methionine
 874 gamma-lyase from *Brevibacterium linens* BL2. *Appl Environ Microbiol* **64**:3327-
 875 3331.
- 876 50. **Ali V, Nozaki T.** 2007. Current therapeutics, their problems, and sulfur-
 877 containing-amino-acid metabolism as a novel target against infections by
 878 "amitochondriate" protozoan parasites. *Clin Microbiol Rev* **20**:164-187.
- 879 51. **Dembek M, Barquist L, Boinett CJ, Cain AK, Mayho M, Lawley TD,**
 880 **Fairweather NF, Fagan RP.** 2015. High-throughput analysis of gene essentiality
 881 and sporulation in *Clostridium difficile*. *MBio* **6**:e02383.
- 882 52. **Boudry P, Gracia C, Monot M, Caillet J, Saujet L, Hajnsdorf E, Dupuy B,**
 883 **Martin-Verstraete I, Soutourina O.** 2014. Pleiotropic role of the RNA chaperone
 884 protein Hfq in the human pathogen *Clostridium difficile*. *J Bacteriol* **196**:3234-
 885 3248.
- 886 53. **Neumann-Schaal M, Hofmann JD, Will SE, Schomburg D.** 2015. Time-resolved
 887 amino acid uptake of *Clostridium difficile* 630Deltaerm and concomitant
 888 fermentation product and toxin formation. *BMC Microbiol* **15**:281.
- 889 54. **Hullo MF, Auger S, Dassa E, Danchin A, Martin-Verstraete I.** 2004. The
 890 *metNPQ* operon of *Bacillus subtilis* encodes an ABC permease transporting
 891 methionine sulfoxide, D- and L-methionine. *Res Microbiol* **155**:80-86.
- 892 55. **Rodionov DA, Vitreschak AG, Mironov AA, Gelfand MS.** 2004. Comparative
 893 genomics of the methionine metabolism in Gram-positive bacteria: a variety of
 894 regulatory systems. *Nucleic Acids Research* **32**:3340-3353.
- 895 56. **Soutourina OA, Monot M, Boudry P, Saujet L, Pichon C, Sismeiro O,**
 896 **Semenova E, Severinov K, Le Bouguenec C, Coppee JY, Dupuy B, Martin-**
 897 **Verstraete I.** 2013. Genome-Wide Identification of Regulatory RNAs in the
 898 Human Pathogen *Clostridium difficile*. *PLoS Genet* **9**:e1003493.
- 899 57. **Burguiere P, Auger S, Hullo MF, Danchin A, Martin-Verstraete I.** 2004. Three
 900 different systems participate in L-cystine uptake in *Bacillus subtilis*. *J Bacteriol*
 901 **186**:4875-4884.
- 902 58. **Awano N, Wada M, Mori H, Nakamori S, Takagi H.** 2005. Identification and
 903 functional analysis of *Escherichia coli* cysteine desulhydrases. *Appl Environ*
 904 *Microbiol* **71**:4149-4152.
- 905 59. **Hindson VJ.** 2003. Serine acetyltransferase of *Escherichia coli*: substrate
 906 specificity and feedback control by cysteine. *Biochem J* **375**:745-752.

- 907 60. **Harris CL.** 1981. Cysteine and growth inhibition of *Escherichia coli*: threonine
908 deaminase as the target enzyme. *J Bacteriol* **145**:1031-1035.
- 909 61. **Lee JW, Helmann JD.** 2007. Functional specialization within the Fur family of
910 metalloregulators. *Biometals* **20**:485-499.
- 911 62. **Vasileva D, Janssen H, Honicke D, Ehrenreich A, Bahl H.** 2012. Effect of iron
912 limitation and fur gene inactivation on the transcriptional profile of the strict
913 anaerobe *Clostridium acetobutylicum*. *Microbiology* **158**:1918-1929.
- 914 63. **Ollinger J, Song KB, Antelmann H, Hecker M, Helmann JD.** 2006. Role of the
915 Fur regulon in iron transport in *Bacillus subtilis*. *J Bacteriol* **188**:3664-3673.
- 916 64. **Ho TD, Ellermeier CD.** 2015. Ferric Uptake Regulator Fur Control of Putative
917 Iron Acquisition Systems in *Clostridium difficile*. *J Bacteriol* **197**:2930-2940.
- 918 65. **Torres VJ, Attia AS, Mason WJ, Hood MI, Corbin BD, Beasley FC, Anderson
919 KL, Stauff DL, McDonald WH, Zimmerman LJ, Friedman DB, Heinrichs DE,
920 Dunman PM, Skaar EP.** 2010. *Staphylococcus aureus* fur regulates the
921 expression of virulence factors that contribute to the pathogenesis of pneumonia.
922 *Infect Immun* **78**:1618-1628.
- 923 66. **Nielsen AH, Hvitved-Jacobsen T, Vollertsen J.** 2008. Effects of pH and iron
924 concentrations on sulfide precipitation in wastewater collection systems. *Water
925 Environ Res* **80**:380-384.
- 926 67. **Jackson S, Calos M, Myers A, Self WT.** 2006. Analysis of proline reduction in the
927 nosocomial pathogen *Clostridium difficile*. *J Bacteriol* **188**:8487-8495.
- 928 68. **Kim SH, Schneider BL, Reitzer L.** 2010. Genetics and regulation of the major
929 enzymes of alanine synthesis in *Escherichia coli*. *J Bacteriol* **192**:5304-5311.
- 930 69. **Vitreschak AG, Mironov AA, Lyubetsky VA, Gelfand MS.** 2008. Comparative
931 genomic analysis of T-box regulatory systems in bacteria. *RNA* **14**:717-735.
- 932 70. **Brinsmade SR, Kleijn RJ, Sauer U, Sonenshein AL.** 2010. Regulation of CodY
933 activity through modulation of intracellular branched-chain amino acid pools. *J
934 Bacteriol* **192**:6357-6368.
- 935 71. **Fonknechten N, Chaussonnerie S, Tricot S, Lajus A, Andreesen JR, Perchat N,
936 Pelletier E, Gouyvenoux M, Barbe V, Salanoubat M, Le Paslier D,
937 Weissenbach J, Cohen GN, Kreimeyer A.** 2010. *Clostridium sticklandii*, a
938 specialist in amino acid degradation: revisiting its metabolism through its genome
939 sequence. *BMC Genomics* **11**:555.
- 940 72. **Troxell B, Hassan HM.** 2013. Transcriptional regulation by Ferric Uptake
941 Regulator (Fur) in pathogenic bacteria. *Front Cell Infect Microbiol* **3**:59.
- 942 73. **Dalet K, Briand C, Cenatiempo Y, Hechard Y.** 2000. The rpoN gene of
943 *Enterococcus faecalis* directs sensitivity to subclass IIa bacteriocins. *Curr
944 Microbiol* **41**:441-443.
- 945 74. **Iyer VS, Hancock LE.** 2012. Deletion of sigma(54) (rpoN) alters the rate of
946 autolysis and biofilm formation in *Enterococcus faecalis*. *J Bacteriol* **194**:368-
947 375.
- 948 75. **Mattila M, Somervuo P, Rattei T, Korkeala H, Stephan R, Tasara T.** 2012.
949 Phenotypic and transcriptomic analyses of Sigma L-dependent characteristics in
950 *Listeria monocytogenes* EGD-e. *Food Microbiol* **32**:152-164.
- 951 76. **Okada Y, Okada N, Makino S, Asakura H, Yamamoto S, Igimi S.** 2006. The
952 sigma factor RpoN (sigma54) is involved in osmotolerance in *Listeria
953 monocytogenes*. *FEMS Microbiol Lett* **263**:54-60.

- 954 77. **Saldias MS, Lamothe J, Wu R, Valvano MA.** 2008. Burkholderia cenocepacia
 955 requires the RpoN sigma factor for biofilm formation and intracellular trafficking
 956 within macrophages. *Infect Immun* **76**:1059-1067.
- 957 78. **Francke C, Groot Kormelink T, Hagemeijer Y, Overmars L, Sluijter V,**
 958 **Moezelaar R, Siezen RJ.** 2011. Comparative analyses imply that the enigmatic
 959 Sigma factor 54 is a central controller of the bacterial exterior. *BMC Genomics*
 960 **12**:385.
- 961 79. **Fried L, Behr S, Jung K.** 2013. Identification of a target gene and activating
 962 stimulus for the YpdA/YpdB histidine kinase/response regulator system in
 963 *Escherichia coli*. *J Bacteriol* **195**:807-815.
- 964 80. **Paczia N, Nilgen A, Lehmann T, Gatgens J, Wiechert W, Noack S.** 2012.
 965 Extensive exometabolome analysis reveals extended overflow metabolism in
 966 various microorganisms. *Microb Cell Fact* **11**:122.
- 967 81. **Yangtse W, Zhou Y, Lei Y, Qiu Y, Wei X, Ji Z, Qi G, Yong Y, Chen L, Chen S.** 2012.
 968 Genome sequence of *Bacillus licheniformis* WX-02. *J Bacteriol* **194**:3561-3562.
- 969 82. **Arous S, Buchrieser C, Folio P, Glaser P, Namane A, Hebraud M, Hechard Y.**
 970 2004. Global analysis of gene expression in an rpoN mutant of *Listeria*
 971 *monocytogenes*. *Microbiology* **150**:1581-1590.
- 972 83. **Koenigsnecht MJ, Theriot CM, Bergin IL, Schumacher CA, Schloss PD, Young**
 973 **VB.** 2015. Dynamics and establishment of *Clostridium difficile* infection in the
 974 murine gastrointestinal tract. *Infect Immun* **83**:934-941.
- 975 84. **Keeney KM, Finlay BB.** 2011. Enteric pathogen exploitation of the microbiota-
 976 generated nutrient environment of the gut. *Curr Opin Microbiol* **14**:92-98.
- 977 85. **Gantois I, Ducatelle R, Pasmans F, Haesebrouck F, Hautefort I, Thompson A,**
 978 **Hinton JC, Van Immerseel F.** 2006. Butyrate specifically down-regulates
 979 salmonella pathogenicity island 1 gene expression. *Appl Environ Microbiol*
 980 **72**:946-949.
- 981 86. **Huang Y, Suyemoto M, Garner CD, Cicconi KM, Altier C.** 2008. Formate acts as
 982 a diffusible signal to induce *Salmonella* invasion. *J Bacteriol* **190**:4233-4241.
- 983 87. **Hussain, H.A, A.P, Robert and P. Mullany** Generation of an erythromycin-
 984 sensitive derivative of *Clostridium difficile* strain 630 (630Deltaerm) and
 985 demonstration that the conjugative transposon Tn916DeltaE enters the genome of
 986 this strain at multiple sites. *J Med Microbiol.* **54**:137-41.
- 987 88. **O'Connor, J. R., D. Lyras, K. A. Farrow, V. Adams, D. R. Powell, J. Hinds, J. K.**
 988 **Cheung, and J. I. Rood.** 2006. Construction and analysis of chromosomal
 989 *Clostridium difficile* mutants. *Mol. Microbiol.* **61**:1335-1351.
- 990
 991
 992
 993
 994

995 **Tables and figures**

996

997 **Figure 1. Schematic overview of sulfur metabolism in bacteria**

998 APS, adenylyl sulfate; OAS, *O*-acetylserine; OAH, *O*-acetylhomoserine; SAM, S-adenosyl-
999 methionine.

1000

1001 **Figure 2. Effect of cysteine on toxin production in different *C. difficile* strains**

1002 A) Cytotoxicity assays on Vero cells. Two-fold serial dilutions of intracellular bacterial
1003 crude extracts were performed, and the dilutions were added to a 96-well plate of
1004 confluent Vero cells. The toxin titer corresponds to the lowest dilution of *C. difficile* crude
1005 extracts required for > 50 % cell rounding. Cytotoxicity results are presented as the ratio
1006 of the toxin titers of bacterial cells grown in the presence of cysteine (PYC) to those of
1007 bacterial cells grown in the absence of cysteine (PY). B) TcdA dot-blot analysis. The crude
1008 extracts of *C. difficile* strains (200 ng for strains 630 Δ *erm*, M7404 and M7404
1009 complemented with pDLL17-*tcdC* and 20 ng for strain VPI10463) were probed with anti-
1010 TcdA antibodies as described in the materials and methods section. The results presented
1011 are representative of crude extracts tested from at least three independent experiments.
1012 C) Transcript levels of *tcdR*, *tcdA* and *tcdB* genes in strain 630 Δ *erm* grown in the presence
1013 or absence of cysteine. . results are presented as the ratio of the mRNA level (arbitrary
1014 units) of each gene in bacterial cells grown in the presence of cysteine (PYC) to that of
1015 each gene in cells grown in the absence (PY) of cysteine. The results are the averages of at
1016 least three independent experiments (error bars are the standard deviations from the
1017 mean values). The statistical analysis was performed by using a t-test (*tcdA*, *tcdR*) or a
1018 Mann-Whitney test (*tcdB*).

1019

1020 **Figure 3. Reconstruction of sulfur metabolism in *C. difficile***

1021 Genes of strain 630 Δ *erm* are renamed on the basis of *B. subtilis* orthologs. *cysE*: serine *O*-
1022 acetyltransferase (CD1595); *cysK*: OAS-thiol-lyase (CD1594); *asrABC*: anaerobic sulfite
1023 reductase (CD2231-2233); *ssuCBA₁*: ABC-transport system sulfonates (CD1482-1484);
1024 *ssuCBA₂*: ABC-transport system sulfonates (CD2989-2991); *metA*: homoserine acetyl-
1025 transferase (CD1826); *metY*: OAH thiol-lyase (CD1825); *maly*: cystathionine β -lyase
1026 (CD3029); *metH*: cobalamin-dependent methionine synthase (CD3596); *metK*: SAM
1027 synthetase (CD0130); *mtnN*: adenosylhomocysteine nucleosidase (CD2611); *luxS*: S-
1028 ribosylhomocysteine lyase (CD3598); *mdeA*: methionine γ -lyase (CD3577), *metNIQ₁*: ABC-

1029 transport system methionine (CD1489-1491); *pepT*, peptidase T (CD1046); *pepA*, leucine
1030 aminopeptidase (CD1300); AI-2, autoinducer 2; OAS; *O*-acetylserine; OAH, *O*-
1031 acetylhomoserine SAM, S-adenosyl-methionine; SAH, S-adenosyl-homocysteine; SRH, S-
1032 ribosyl-homocysteine. Ext means “external”. As indicated, an S-box motif is located
1033 upstream of the *metY-metA* and *metNIQ₁* operons and of the *metQ₂* and *metK* genes,
1034 suggesting that they are controlled by a SAM-dependent riboswitch (55). A Tbox is
1035 present upstream of *hom-CD1580*.

1036

1037 **Figure 4. Hydrogen sulfide production in strain 630Δerm.**

1038 A) Detection of H₂S production using lead-acetate paper. H₂S production was evaluated in
1039 PY, PY plus cysteine (PYC) and PY plus homocysteine (PYHC) media. The production of
1040 H₂S yielded a black color due to the formation of PbS. B) Detection of the homocysteine g-
1041 lyase activity on a zymogram. Crude extracts of strain 630Δerm grown in PY, PYC or PYHC
1042 were loaded on a native polyacrylamide gel (12 %) and incubated with 10 mM
1043 homocysteine. Homocysteine γ-lyase was detected by the formation of insoluble PbS via
1044 the release of H₂S. Lanes of the zymogram have been reorganized from the same image to
1045 present data chronologically. C) Quantitative detection of H₂S after 6 h or 10 h of growth
1046 of strain 630Δerm in PY (white boxes) or PYC (black boxes). H₂S production was
1047 measured using the quantitative methylene blue method, as described in the materials
1048 and methods section. The statistical analysis was performed by using Mann-Whitney test
1049 for all genes. D) Detection of cysteine desulhydrase activities on a zymogram. Crude
1050 extracts of strain 630Δerm (lane 1 and lane 2), 630Δerm::*cysK* (lane 3), 630Δerm::*sigL*
1051 (lane 4), 630Δerm + pRPF185 (lane 5) and 630Δerm + pDIA6456-AS*malY* (lane 6). The
1052 strains were grown in PY (lane 1) or PYC (lane 2 to 6). Samples were charged on a native
1053 polyacrylamide gel (12 %) and incubated with 10 mM cysteine. The cysteine
1054 desulhydrases were detected by the formation of insoluble PbS formed by the release of
1055 H₂S. The results presented are representative of at least three independent experiments.
1056 Lanes of the zymogram have been reorganized from the same image to present data
1057 chronologically

1058

1059 **Figure 5. Analysis of Fur-regulated genes induced in the presence of cysteine**

1060 A) Consensus sequence of the Fur box motif of *C. difficile*. The sequence logo was created
1061 by the alignment of putative Fur-regulated genes induced in the presence of cysteine on

1062 the Weblogo website (<http://weblogo.berkeley.edu>). The height of the nucleotides is
 1063 proportional to their frequency B) Effect of cysteine on the transcript level of *fur*
 1064 (CD1287), *feoB1* (CD1479), *cysK* (CD1594), *fhuD* (CD2878) and *CD2992* in *630Δerm* and
 1065 the *630Δerm::fur*. The *630Δerm* (white boxes) and *630Δerm::fur* (black boxes) strains
 1066 were grown for 10 h in PY or PYC. qRT-PCR results are presented as the ratio of the
 1067 amount of mRNA (arbitrary units) of each gene in bacterial cells grown in PYC to that of
 1068 each mRNA in the bacterial cells grown in PY. Data are the averages of at least three
 1069 independent experiments (error bars are the standard deviations from the mean values).
 1070 C) Aspect of the bacterial pellet of strain *630Δerm* grown for 10 h in PY or in PYC. The
 1071 black precipitate is due to FeS precipitation.

1072
 1073 **Figure 6. Overview of *C. difficile* genes involved in carbon and amino acid
 1074 metabolism that are differentially expressed in the presence of cysteine.** Genes that

1075 are up- and down-regulated in the presence of cysteine in the transcriptome analysis are
 1076 indicated in red and green, respectively. "*" means that the differential transcript level
 1077 was detected by qRT-PCR. A) Carbon metabolism and fermentation pathways.
 1078 Assignments of genes regulated by cysteine availability are as follows: *tpi*,
 1079 triosephosphate isomerase; *gapA/gapN*, glyceraldehyde-3-phosphate dehydrogenase;
 1080 *pgk*, phosphoglycerate kinase; *pgm*, 2,3-bisphosphoglycerate-mutase; *celABC*, PTS
 1081 cellobiose; *celF*, cellobiose-6-P hydrolase; *ldh*, lactate dehydrogenase; *adhE*, aldehyde-
 1082 alcohol dehydrogenase; *pflB* and *pflD*, pyruvate formate lyase; *pflE* and *pflA*, pyruvate
 1083 formate lyase activating enzyme; *thiA1*, acetyl-CoA acetyltransferase; *bcd2*, butyryl-CoA
 1084 dehydrogenase; *hbD2*, 3-hydroxybutyryl-CoA dehydrogenase; *crt2*, 3-hydroxybutyryl-CoA
 1085 dehydratase; *buk*, butyrate kinase; *malY*, cysteine desulfhydrase; *ilvD*, dihydroxy-acid
 1086 dehydratase; *leuA*, 2-isopropylmalate synthase; *leuB*, 3-isopropylmalate dehydrogenase;
 1087 *leuC*, 3-isopropylmalate dehydratase large subunit; *leuD*, 3-isopropylmalate dehydratase
 1088 small subunit; *brnQ1*, BCAA transporter. B) Stickland reactions and associated
 1089 metabolism. Assignments of genes regulated in response to cysteine availability are as
 1090 follows: *grdDCBAEX*, glycine reductase complex; *prdEDBA*, proline reductase; *prdF*,
 1091 proline racemase; *CD2347*, putative Xaa-Pro dipeptidase; *proC*, pyrroline-5-carboxylate
 1092 reductase, *gcvPB*, glycine decarboxylase; *gcvTPA*, bi-functional glycine
 1093 dehydrogenase/aminomethyl transferase protein.

1094

1095 **Figure 7. Role of Fur, CcpA, CodY and SigL in the cysteine-dependent repression of**
 1096 **toxin production.** Strains JIR8094, JIR8094::*codY* and JIR8094::*ccpA* (A) and strains
 1097 630 Δ *erm*, 630 Δ *erm*::*fur*, 630 Δ *erm*::*sigL* and 630 Δ *erm*::*sigL* + pDIA6309-*sigL* (B) were
 1098 grown for 10 h in PY or PYC. TcdA production was estimated from crude extracts by dot-
 1099 blot analysis using an anti-TcdA antibody. The results are representative of at least three
 1100 independent experiments. C) Effect of cysteine on *tcdA*, *tcdB* and *tcdR* transcript levels in
 1101 630 Δ *erm*::*sigL* (white boxes) or 630 Δ *erm*::*sigL* complemented with pDIA6309-*sigL* (black
 1102 boxes) versus the wild-type strain 630 Δ *erm*. All strains were grown for 10 h in PYC. qRT-
 1103 PCR results are presented as the ratio between the amount of the mRNA (arbitrary units)
 1104 of each gene normalized by the DNA *polIII* gene in both 630 Δ *erm*::*sigL* and 630 Δ *erm*::*sigL*
 1105 complemented with pDIA6309-*sigL* compared to the mRNA level in the wild-type strain.
 1106 Data are the averages of at least three independent experiments (error bars are the
 1107 standard deviations from the mean values). The statistical analysis was performed by
 1108 using a t-test for all genes with an exception for *tcdB* (Mann-Whitney test).

1109

1110 **Figure 8. Effect of *sigL* inactivation on cysteine degradation and pyruvate**
 1111 **production**

1112 A) Detection of H₂S production in the 630 Δ *erm*, 630 Δ *erm*::*sigL* and 630 Δ *erm*::*sigL* +
 1113 pDIA6309-*sigL* strains grown in PYC by using lead-acetate papers. B) Quantitative
 1114 detection of pyruvate in the supernatant of strains 630 Δ *erm*, 630 Δ *erm*::*sigL* and
 1115 630 Δ *erm*::*sigL* + pDIA6309-*sigL* after 10 h of growth in PY (white boxes) or PYC (black
 1116 boxes). The statistical analysis was performed by using Mann-Whitney test for all genes,
 1117 ns: non significant.

1118

1119 **Figure 9. Effect of pyruvate and Na₂S on toxin-gene expression**

1120 A) Transcript levels of *tcdA*, *tcdB* and *tcdR* genes in strain 630 Δ *erm* after 1 h of exposure
 1121 to pyruvate (white boxes) or Na₂S (black boxes). The strain was grown in PY for 9 h, and
 1122 10 mM pyruvate or 10 mM Na₂S was then added to the medium. Cells were centrifuged 1
 1123 h later. The statistical analysis was performed by using a t-test for all genes, with an
 1124 exception for *tcdB*+Na₂S (Mann-Whitney test). B) Transcript levels of the *tcdA*, *tcdB* and
 1125 *tcdR* genes of strain 630 Δ *erm* after 1 h of exposure to formate (white boxes) or acetate
 1126 (black boxes). The strain was grown in PY for 9 h and 10 mM formate or 10 mM acetate
 1127 was then added to the medium and cells were centrifuged 1 h later. The statistical

1128 analysis was performed by using a t-test for all genes, with an exception for *tcdB*+acetate
 1129 (Mann-Whitney test). C) Transcript levels of the *tcdA*, *tcdB* and *tcdR* genes of strain
 1130 630 Δ *erm* (white boxes) and 630 Δ *erm*::*CD2602* (black boxes) after exposure to pyruvate
 1131 for 1 h, as described in panel A. qRT-PCR results are presented as the ratio between the
 1132 amount of mRNA (arbitrary units) of each gene normalized by the DNA *polIII* gene from
 1133 bacterial cells grown in PY supplemented with one of the compounds (pyruvate, Na₂S,
 1134 formate or acetate) compared to the amount of mRNA in the untreated cells. Data are the
 1135 averages of at least three independent experiments (error bars are the standard
 1136 deviations from the mean values). The statistical analysis was performed by using a t-test
 1137 for all genes, with an exception for *tcdR*+pyruvate (Mann-Whitney test).

1138
 1139
 1140

Table 1. Strains and plasmids used in this study.

| strains | background | knockout or overexpressed gene | plasmid | origin |
|------------------------------------|-------------------------|--------------------------------|-------------------------------------|--------------------------------|
| 630 Δ <i>erm</i> | | | | 87 |
| M7404 | BI/NAP1/027 | | | 2 |
| M7404 (<i>tcdC</i> ⁺) | BI/NAP1/027 | | pDLL17 (<i>tcdC</i> ⁺) | 2 |
| VPI10463 | | | | Virginia Polytechnic Institute |
| CDIP001 | 630 Δ <i>erm</i> | <i>CD1287 (fur)::erm</i> | | This study |
| CDIP106 | 630 Δ <i>erm</i> | <i>CD0278::erm</i> | | This study |
| CDIP107 | 630 Δ <i>erm</i> | <i>CD2023::erm</i> | | This study |
| CDIP110 | 630 Δ <i>erm</i> | <i>CD2065::erm</i> | | This study |
| CDIP217 | 630 Δ <i>erm</i> | <i>CD3176 (sigL)::erm</i> | | This study |
| CDIP342 | 630 Δ <i>erm</i> | <i>CD3176 (sigL)::erm</i> | pDIA6309 | This study |
| CDIP540 | 630 Δ <i>erm</i> | <i>CD1594 (cysK)::erm</i> | | This study |
| CDIP656 | 630 Δ <i>erm</i> | | pDIA6456 | This study |
| CDIP657 | 630 Δ <i>erm</i> | <i>CD2602::erm</i> | | This study |
| JIR8094 | | | | 88 |
| CDIP100 | JIR8094 | <i>CD1064 (ccpA)::erm</i> | | 13 |
| LB-CD15 | JIR8094 | <i>CD1275 (codY)::erm</i> | pBL92 | Bouillaut et al., in prep |
| plasmids | vector | cloned gene | resistance | origin |
| pDIA5906 | pMTL007 | Intron <i>CD1287 (fur)</i> | <i>Cm, Tm</i> | This study |
| pDIA6309 | pMTL84121 | <i>CD3176 (sigL)</i> | <i>Cm, Tm</i> | This study |
| pDIA6450 | pMTL007 | Intron <i>CD0278</i> | <i>Cm, Tm</i> | This study |
| pDIA6451 | pMTL007 | Intron <i>CD2065</i> | <i>Cm, Tm</i> | This study |
| pDIA6452 | pMTL007 | Intron <i>CD2023</i> | <i>Cm, Tm</i> | This study |

| | | | | |
|----------|---------|-----------------------------|---------------|------------|
| pDIA6453 | pMTL007 | Intron <i>CD3176</i> | <i>Cm, Tm</i> | This study |
| pDIA6454 | pMTL007 | Intron <i>CD2602</i> | <i>Cm, Tm</i> | This study |
| pDIA6455 | pMTL007 | Intron <i>CD1594 (cysK)</i> | <i>Cm, Tm</i> | This study |
| pDIA6456 | pRPF185 | AS <i>CD3029 (malY)</i> | <i>Cm, Tm</i> | This study |

1141 *Cm* : chloramphenicol; *Tm* : thiamphenicol; *Erm* : Erythromycin; AS : Antisens

1142

1143 **Table 2.** Growth of *C. difficile* strain 630 Δ *erm* in minimal medium containing different sulfur

1144 sources.

1145

| Sulfur source | Growth | |
|----------------------|--------|------|
| | 16 h | 48 h |
| Sulfate (4 mM) | - | - |
| Sulfite (4 mM) | - | - |
| Sulfide (4 mM) | + | + |
| Thiosulfate (4 mM) | - | + |
| Cysteine (4 mM) | + | + |
| Cystine (2 mM) | - | + |
| Glutathione (2 mM) | + | + |
| Cystathionine (2 mM) | - | + |
| Homocysteine (2 mM) | + | + |
| Methionine (1.5 mM) | - | - |

1146 + indicates a growth and – an absence of growth

1147

1148 **Table 3.** List of the Fur-regulon genes that are differentially expressed in PY and PYC with

1149 a putative Fur box in their promoter region.

1150

| Gene | function | Ratio PYC/PY | Fur box |
|----------------------|---|-----------------|---------|
| <i>CD1287 fur</i> | Ferric uptake regulation protein | 3.3 | - 38 |
| <i>CD1477 feoA</i> | Ferrous iron transport protein A | 64.1 | |
| <i>CD1478 feoA1</i> | Ferrous iron transport protein A1 | 107.0 | |
| <i>CD1479 feoB1</i> | Ferrous iron transport protein B1 | 127.1 | - 60 |
| <i>CD1480</i> | putative exported protein | 162.6 | |
| <i>CD1745A feoA</i> | Ferrous iron transport protein A | 16.7 | - 30 |
| <i>CD3273 feoA3</i> | Ferrous iron transport protein A | 13.4 | - 30 |
| <i>FCD3274 feoB3</i> | Ferrous iron transport protein B | 12.1 | |
| <i>CD2878 fluD</i> | ABC transporter, ferrichrome substrate-binding protein; | N/A | - 47 |
| <i>CD2875 fluC</i> | Ferrichrome ABC transporter | 3.0 | |
| <i>CD1594 cysK</i> | <i>O</i> -acetyl-serine sulfhydrylase | 43.0 | - 162 |
| <i>CD1595 cysE</i> | Serine acetyltransferase | 44.0 | |
| <i>CD1999 fldX</i> | Flavodoxin | 28.5 | - 158 |
| <i>CD1777</i> | Putative arsenate reductase | 3.3 | - 80 |
| <i>CD1485</i> | Conserved hypothetical protein | 6.9 | - 34 |
| <i>CD2499</i> | Conserved hypothetical protein | 15.4 | - 34 |
| <i>CD2881</i> | Conserved hypothetical protein | 2.6 | - 58 |

| | | | |
|--------|---|-----|------|
| CD2992 | Conserved hypothetical protein, | 2.5 | |
| CD2991 | ABC transporter, sulfonate-permease | 3.5 | - 36 |
| CD2989 | ABC transporter, sulfonate-extracellular solute-binding protein | 4.8 | |

1151

1152 The position of the Fur box is indicated according to the translational start site of the
 1153 corresponding gene. N/A means “not detected in transcriptome”.

1154

1155

1156 **Table 4.** Effect of cysteine addition on the intracellular concentration of amino acids in strain
 1157 630Δ*erm*.

1158

| Amino-acids | PY (μmol/L) | PYC (μmol/L) | Ratio PYC/PY |
|---|---------------|----------------|--------------|
| Up in the presence of cysteine | | | |
| Leucine | ND | 16.25 +/- 1.6 | + |
| Tyrosine | ND | 20 +/- 1.2 | + |
| Alanine | 13.5 +/- 0.7 | 748 +/- 40 | 55 |
| Valine | 5.3 +/- 0.5 | 56.8 +/- 1.3 | 10 |
| Phenylalanine | 2.6 +/- 0.5 | 25.75 +/- 5 | 10 |
| Glutamic acid | 19.3 +/- 2 | 121.9 +/- 9.5 | 6.5 |
| Aminobutyric acid | 8.5 +/- 0.5 | 46.35 +/- 0.8 | 5.5 |
| Threonine | 1.1 +/- 0.1 | 2.4 +/- 0.4 | 2.2 |
| Serine | 4 +/-0 | 9.85 +/- 0.15 | 2.5 |
| Asparagine | 29.7 +/-2.6 | 59.7 +/-1.6 | 2 |
| Methionine | 4.85 +/- 0.35 | 11.65 +/- 1.65 | 2.5 |
| Down in the presence of cysteine | | | |
| Cystathionine | 1.2 +/- 0.2 | ND | - |
| Glutamine | 11.8 +/- 0.4 | 6 +/-0.1 | 0.5 |
| Hydroxyproline | 23.3 +/- 1.5 | 13.9 +/-0.5 | 0.6 |

1159 ND means not detectable

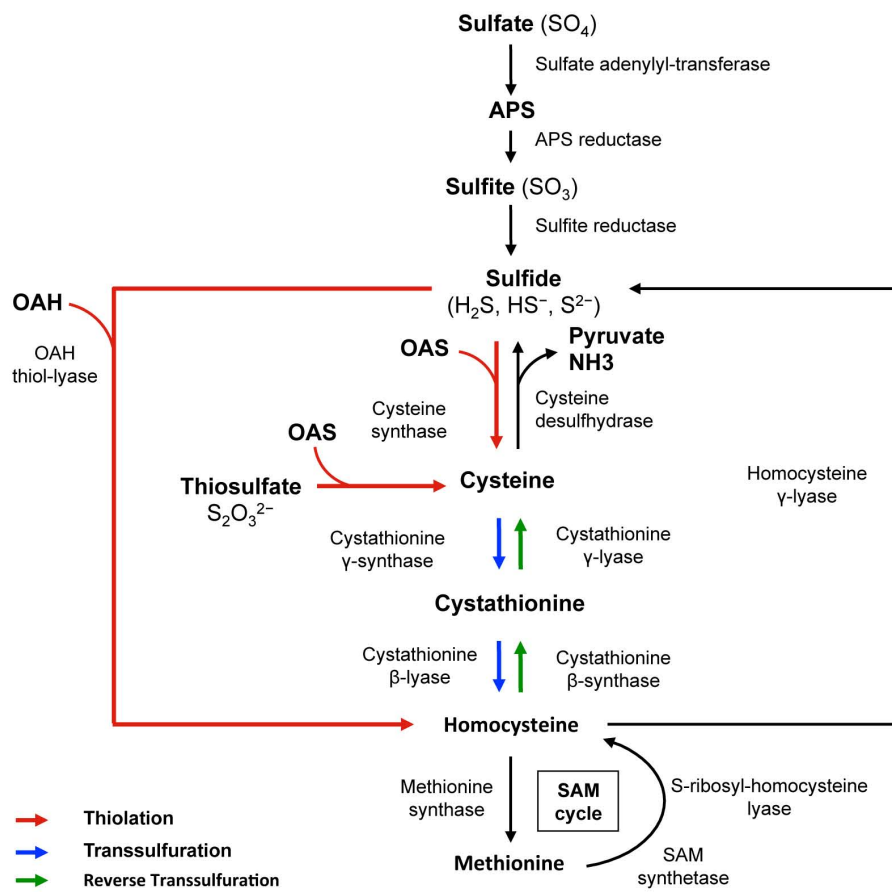


Fig. 1

A

| | 630 Δ <i>erm</i> | M7404 | M7404 (<i>tcdC</i> ⁺) | VPI10463 |
|--------|-------------------------|---------------------------------------|---------------------------------------|---------------------|
| PYC/PY | $4 \cdot 10^{-2}$ | $4 \cdot 10^{-2}$ - $8 \cdot 10^{-3}$ | $4 \cdot 10^{-2}$ - $8 \cdot 10^{-3}$ | $6.3 \cdot 10^{-5}$ |

